Supporting Information

Combined Effect of Ether and Siloxane Substituents on Imidazolium Ionic Liquids

Santosh N. Chavan, and Debaprasad Mandal*

Department of Chemistry, Indian Institute of Technology Ropar
Punjab 140001, India, E-mail: dmandal@iitrpr.ac.in

Preparation of 1-(chloromethyl)-1,1,3,3,3-pentamethyl disiloxane (6a) (Scheme S1)**:** (Modified)[1] A RB flask was charged with Chloromethyldimethylchlorosilane (7.604 g, 70.00 mmol). Trimethylsilylchloride (10.016 g, 70.00 mmol) and deionized water (7.0 mL, 388.9 mmol) was added simultaneously drop wise at 0 °C. Cooling bath was removed and the mixture was stirred for 0.5 h. Anhydrous Na_2CO_3 (10.012 g, 94.35 mmol) was added portion wise with stirring and then filtered. Distilled this limpid solution by fractional distillation and obtained three pure products at different boiling points; **6a** at 50-80 °C (0.1 mmHg) (5.457 g, 27.72 mmol) and **7a** at 140 °C (0.1 mmHg) (6.245g, 27.00 mmol).

Preparation of 1-(iodomethyl)-1,1,3,3,3-pentamethyl disiloxane (6)[2] (Scheme S1): A Schlenk flask was charged with anhydrous NaI (4.497 g, 30.00 mmol), Aliquat 336 (0.181 g, 0.45 mmol, 2.25 mol%), dry acetone (60 mL), and **6a** from last step (5.560 g, 28.25 mmol). The reaction mixture was refluxed for 4 h. The mixture was filtered through G4 frit by avoiding moisture and maximum acetone was evaporated in vacuum. The filtrate was distilled by fractional distillation under reduced pressure at 0.1 mmHg. Compound **6** was collected between 60 to 70 °C (0.1 mmHg) (3.257 g, 11.30 mmol, 40%), and **7** at 100 to 130 °C (0.1 mmHg) (1.172g, 2.82 mmol, 10%).

Preparation of 1-(iodomethyl)-1,1,3,3,3-pentamethyl disiloxane (6)[2] (Scheme S1)**:** (Modified one pot procedure) A RB flask was charged with Chloromethyldimethylchlorosilane (7.604 g, 70.00 mmol). Trimethylsilylchloride (10.016 g, 70.00 mmol) and deionized water (7.0 mL, 388.9 mmol) was added simultaneously drop wise at 0 °C. Cooling bath was removed and the mixture was stirred for 0.5 h. After completion, the mixture was dried over anhydrous Na_2CO_3 (10.012 g, 94.35 mmol), filtered and transferred to a Schlenk flask. The Schlenk flask was charged with anhydrous NaI (15.675 g, 105.00 mmol), Aliquat 336 (0.181 g, 0.45 mmol, 2.25 mol%), dry acetone (60 mL), and refluxed for 4 h. The mixture was filtered through G4 frit by avoiding moisture and then maximum acetone was evaporated in vacuum. The filtrate was distilled by fractional distillation under reduced pressure at 0.1 mmHg.

Compound **6** was collected between 60 to 70 °C (0.1 mmHg) (8.698 g, 30.17 mmol, 43%), and **7** at 100 to 130 °C (0.1 mmHg) (11.256 g, 27.17 mmol, 39%).

NMR: (^{1}H, $CDCl_3$) δ ppm: 1.98 (s, 2H, SiCH_2), 0.24 (s, 6H, Si(CH_3)$_2$), 0.10 (s, 9H, Si(CH_3)$_3$). (^{13}C {^{1}H}, $CDCl_3$) δ ppm: 2.07 (s, SiCH_2), -0.26 (s, Si(CH_3)$_2$), -12.13 (s, Si(CH_3)$_3$). (^{29}Si {^{1}H}, $CDCl_3$) δ ppm: 9.64 (s, *Si*(CH_3)$_2$), 3.26 (s, *Si*(CH_3)$_3$).

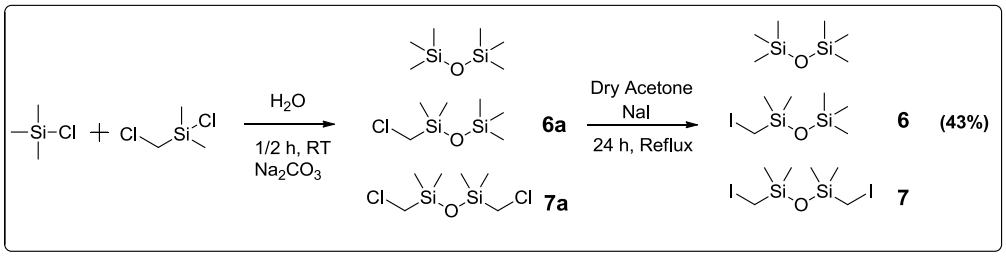

Scheme S1. Preparation of 1-(iodomethyl)-1,1,3,3,3-pentamethyl disiloxane

Preparation of 2-methoxyethyl 4-methylbenzenesulfonate (8) (Scheme S2)[3]**:** A 1000 mL RB flask was charged with 2-methoxyethanol (15.220 g, 200.00 mmol) and 200 mL ethyl acetate, followed by triethylamine (27.8 mL, 200.00 mmol). The reaction mixture stirred at ambient temperature for 1 h. *p*-toluene sulfonyl chloride (39.799 g, 208.80 mmol) was added by pinch. Immediately, a copious precipitate formed and mixture was stirred for 8 h under N_2 at ambient temperature. The reaction progress was checked by TLC in 30% ethyl acetate in hexane. After completion the reaction mixture was filtered and maximum ethyl acetate was evaporated in rotary evaporator and 120 mL water was added. The filtrate was extracted with dichloromethane (100 mL × 3), organic phase was dried over Na_2SO_4 and evaporated to give yellow oil. The yellow oil was purified by flash column chromatography to afforded, (42.371 g, 183.98 mmol, 92%) colorless liquid (**6**).

NMR: (^{1}H, $CDCl_3$) δ ppm: 7.80 (d, *J*=8.3 Hz, 2H, *Ar*-C*H*C*H*), 7.34 (d, *J*=8.0 Hz, 2H, *Ar*-C*H*C*H*), 4.14 (t, *J*=4.8 Hz, 2H, SOCH_2CH_2O), 3.56 (t, *J*=5.0 Hz, 2H, SOCH_2CH_2O), 3.29 (s, 3H, OCH_3), 2.43 (s, 3H, *Ar*-CH_3). **(^{13}C {^{1}H}, $CDCl_3$)** δ ppm: 129.33 (s, *Ar*-2*C*-S), 126.06 (s, *Ar*-2*C*H-CH-C), 69.99 (s, SCH_2CH_2O), 69.19 (s, SC$H_2$$CH_2$O), 59.10 (s, O$CH_3$), 21.10 (s, *Ar*-$CH_3$).

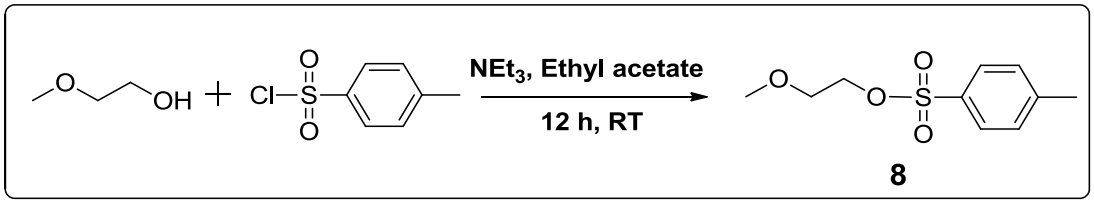

Scheme S2. Synthesis of 2-methoxyethyl-4-methylbenzenesulfonate

2-(2-methoxyethoxy)ethyl 4-methylbenzenesulfonate[3] (9): The 1000 mL RB was charged with 2-(2-methoxyethoxy)ethanol (23.8 mL, 175.00 mmol), 200 mL of THF and followed by powdered NaOH (7.200 g, 180.00 mmol). The reaction was stirred at ambient temperature for 1 h. *p*-toluene sulphonyl chloride (42.504 g, 223.00 mmol) was added by pinch. Immediately, a copious precipitate formed and mixture was refluxed under N_2 for 24 h. The reaction progress was checked by TLC in 30% ethyl acetate in hexane. After completion the reaction mixture was filtered and maximum THF was evaporated in *rotavac.* The filtrate was extracted with dichloromethane (100 mL × 3) and organic phase was dried on Na_2SO_4. Solvent evaporated to give yellow oil and purified by flash column chromatography. Afforded pure colorless liquid (41.278 g, 150.48 mmol, 86%) as shown in Scheme S3.

NMR: (^{1}H, $CDCl_3$) δ ppm: 7.79 (d, *J*=8.3 Hz, 2H, *Ar*-C*H*C*H*), 7.33 (d, *J*=8.0 Hz, 2H, *Ar*-C*H*C*H*), 4.15 (t, *J*=4.8 Hz, 2H, SOCH_2CH_2O), 3.68 (t, *J*=5.0 Hz, 2H, SOCH$_2$CH_2O), 3.60 – 3.51 (m, 2H, OCH_2CH_2O), 3.49 – 3.42 (m, 2H, OCH$_2$CH_2O), 3.34 (s, 3H, OCH_3), 2.44 (s, 3H, *Ar*-CH_3). **(^{13}C {^{1}H}, $CDCl_3$)** δ ppm: 144.79 (s, *Ar*-*C*-S), 132.86 (s, *Ar*-*C*H-*C*H-S), 129.77 (s, *Ar*-*C*H-CH-C), 127.87 (s, *C*-C=CH-*C*H), 71.70 (s, S*C*H$_2$CH$_2$O), 70.53 (s, SCH$_2$*C*H$_2$O), 69.22 (s, O*C*H$_2$CH$_2$O), 68.58 (s, OCH$_2$*C*H$_2$O), 58.91 (s, O*C*H$_3$), 21.53 (s, *Ar*-*C*H$_3$).

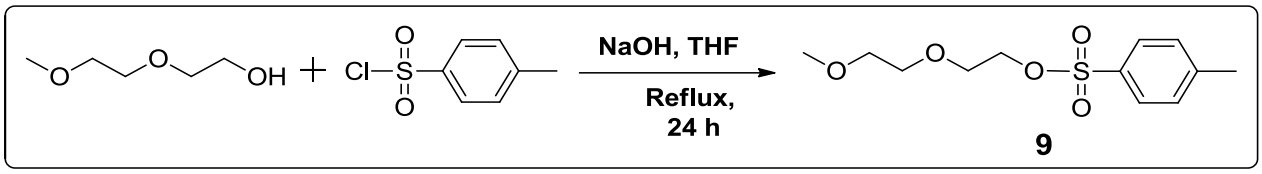

Scheme S3. Synthesis of 2-(2-methoxyethoxy) ethyl-4-methylbenzenesulfonate

Preparation of 1-iodo-2-methoxyethane[4] (10) (Scheme S4): A 1000 mL RB flask was charged with sodium iodide (30.235 g, 201.715 mmol), 200 mL dry acetone, **8** (38.709 g, 168.09 mmol) and phase transfer catalyst Aliquat 336 (0.213 g, 0.52 mmol, 0.31 mol%), The reaction mixture was refluxed under inert atmosphere for 12 h. The reaction progress was checked by thin layer chromatography technique. After completion, the reaction mixture was filtered and evaporated the acetone mixture to minimum under *rotavac*. Then the slurry was extracted from dichloromethane and distilled water (100 mL × 3) and finally the organic phase was washed with 50% $Na_2S_2O_3$ aqueous solution. The organic phase was dried over Na_2SO_4 gives (**10**) yellow liquid (25.014 g, 134.49 mmol, 80%) on evaporation of organic solvent. The obtained liquid distilled under reduced pressure at 120 °C/50 mbar.

NMR: (^{1}H, $CDCl_3$) δ ppm: 3.65 (t, *J*=7.5 Hz, 2H, ICH_2CH$_2$), 3.39 (s, 3H, OCH_3), 3.25 (t, *J*=7.5 Hz, 2H, ICH$_2$CH_2O).

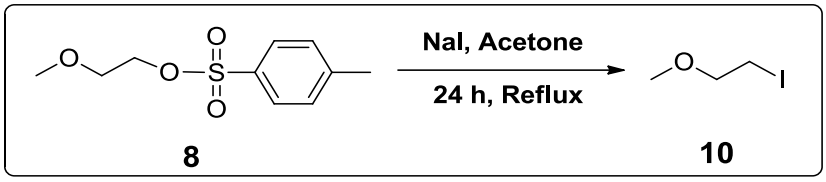

Scheme S4. Preparation of 1-iodo-2-methoxyethane

Preparation of 1-(2-methoxyethyl)-1H-imidazole (1b)[5] **and 1-(2-(2-methoxyethoxy)ethyl)-1H-imidazole (2b)**[6] (Scheme S5): A mixture of imidazole (1.021 g, 15 mmol), NaOH solution (0.7198 g, 18.00 mmol) in THF (17 mL) and **8** (3.454 gm, 15.00 mmol) / **9** (4.114 g, 15.00 mmol) was refluxed for two days. Reaction progress was checked by thin layer chromatography in 60% ethyl acetate in hexane. On completion, the reaction mixture was filtered and evaporated the solvent to minimum in *rotavac*. The mixture was extracted with dichloromethane (50 mL × 3) and water (50 mL). The combined organic layer was washed with water and dried over anhydrous Na_2SO_4. Solvent was removed under reduced pressure gives yellow liquid of (**1b**) (1.614 gm, 12.78 mmol, 85.20%) / **2b** (1.89 g (11.11 mmol, 74.06%). The purification of **1b** was done by fractional distillation at 130 °C / 0.1 mbar and **2b** purified by flash column chromatography.

NMR (1b): (^{1}H, $CDCl_3$) δ ppm: 7.50 (s, 1H, NC*H*N), 7.03 (s, 1H, NC*H*CHN), 6.96 (s, 1H, NCHC*H*N), 4.08 (t, *J*=5.2 Hz, 2H, NCH_2CH_2O), 3.62 (t, *J*=5.2 Hz, 2H, NCH$_2$CH_2O), 3.33 (s, 3H, OCH_3).

NMR (2b): (^{1}H, $CDCl_3$) δ ppm: 7.53 (s, 1H, NC*H*N), 7.03 (s, 1H, NC*H*CHN), 6.98 (s, 1H, NCHC*H*N), 4.11 (t, *J*=5.3 Hz, 2H, NCH_2CH_2O), 3.73 (t, *J*=5.4 Hz, 2H, NCH$_2$CH_2O), 3.58 – 3.54 (m, 2H, OCH_2CH$_2$O), 3.52 – 3.48 (m, 2H, OCH$_2$CH_2O), 3.36 (s, 3H, OCH$_3$). **(^{13}C {^{1}H}, $CDCl_3$)** δ ppm: 137.85 (s, N*C*HN), 129.37 (s, N*C*HCHN), 119.52 (s, NCH*C*HN), 71.97 (s, N*C*H$_2$CH$_2$O), 70.81 (s, NCH$_2$*C*H$_2$O), 70.14 (s, O*C*H$_2$CH$_2$O), 59.22 (s, OCH$_2$*C*H$_2$O), 47.14 (O*C*H$_3$).

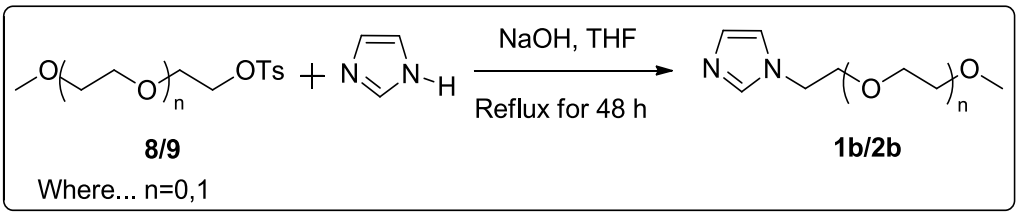

Scheme S5. Preparation of 1-(2-methoxyethyl)-1H-imidazole and 1-(2-(2-methoxyethoxy) ethyl)-1H-imidazole

Preparation of 1-((trimethylsilyl)methyl)-1H-imidazole (4b) (Scheme S6): A dissolved KOH (1.223 g, 20.00 mmol) of 25 mL DMSO taken in 150 mL RB. The imidazole (1.364 g, 20.00 mmol) was added into reaction mixture at 10 °C with vigorous stirring. The stirring continued for 30 min, the temperature during the stirring not exceed then 20 °C. The (chloromethyl)trimethylsilane (2.454 gm, 20.00 mmol) was added in the reaction mixture at the 10 °C. The two drop of phase transfer catalyst Aliquat 336 (0.240 gm, 0.60 mmol, 2.96 mol%) was added into reaction mixture. The reaction mixture stirred for 8 h at ambient temperature. The reaction progress was checked by TLC 60 % ethyl acetate/hexane. After completion of reaction the reaction mixture was extracted with distilled water (50 mL × 7) and diethyl ether. The organic layer was washed with water and dried over anhydrous Na_2SO_4. Solvent was removed under *roatavac*. The residue was distilled under high vacuum (0.01 mbar, 170-180 °C) afford pure colorless liquid **4b** (2.653 g, 17.20 mmol, 86%).

NMR: (^{1}H, $CDCl_3$) δ ppm: 7.34 (s, 1H, NC*H*N), 7.02 (s, 1H, NC*H*CHN), 6.79 (s, 1H, NCHC*H*N), 3.51 (s, 2H, NCH_2Si), 0.08 (s, 9H, Si(CH_3)$_3$). **(^{13}C {^{1}H}, $CDCl_3$)** δ ppm: 136.74 (s, N*C*HN), 128.41 (s, N*C*HCHN), 119.34 (s, NCH*C*HN), 38.09 (s, N*C*H_2Si), –3.27 (s, Si(*C*H_3)$_3$). **(^{29}Si {^{1}H}, $CDCl_3$)** δ ppm: –135.89 (s, *Si*(CH_3)$_3$).

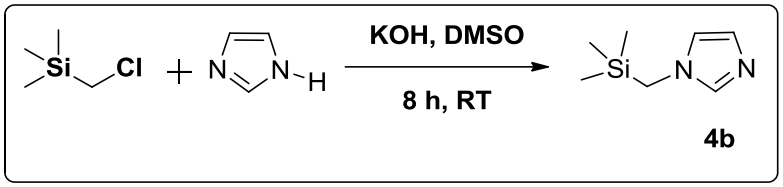

Scheme S6. Preparation of 1-((trimethylsilyl)methyl)-1H-imidazole

Density: The density of ILs (**1-5**) taken from 20 to 40 °C with temperature rise in inert atmosphere. And given in Figure S1.

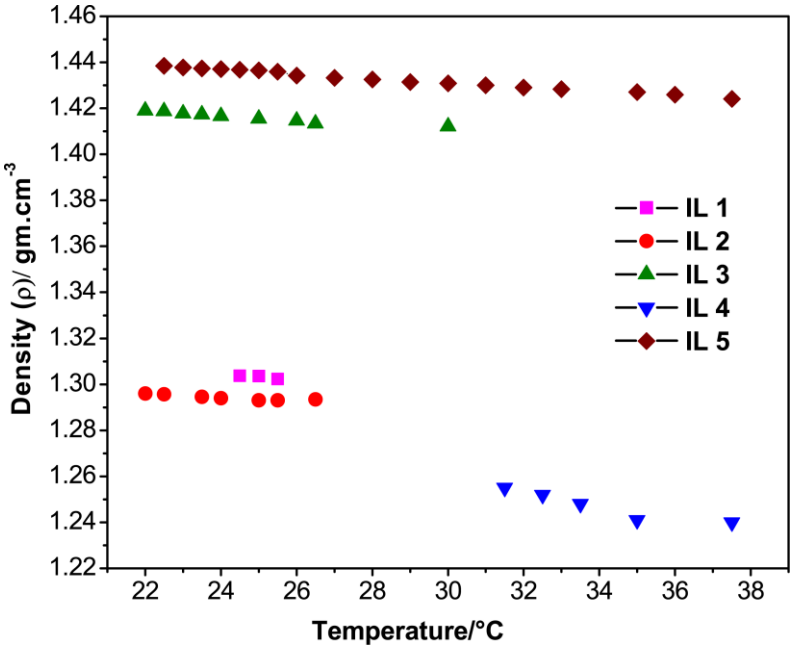

Figure S1. Plot of density *vs*. Temperature for ILs **1-5**.

Viscosity:

Table S1. Literature comparison between ILs **1-5** and [Me-Im-Substituted] TFSI ILs.

IL	1O2-Im-1SiOSi TFSI (**1**)	1O2O2-Im-1SiOSi TFSI (**2**)	1O2O2-Im-2O1 TFSI (**3**)	Si1-Im-1SiOSi TFSI (**4**)	BMIM TFSI (**5**)	Me-Im-2O1 TFSI	Me-Im-2O2O1 TFSI	Me-Im-1SiOSi TFSI	Heptyl-Im-Me TFSI
Mol. Wt. (gm/mol)	567.67	**611.72**	509.07	595.80	419.36	421.34	**465.39**	523.62	461.44
Mol. Vol (m/ρ)	435.46	473.10	359.63	483.56	291.93	288.10	279.34	~404	344.35
Density at 25 °C (gm/cm^3)	1.3036	1.2935	1.4155	1.2520	1.4365	1.5088	1.3036	….	1.34
Viscosity at 25 °C (mPa.s)	**81.9**	**74.7**	**71.9**	**144.5**	**52.3**	**49.6**	**70.3**	**75.6**	75.23

All five ILs viscosity and temperature follows the Vogel–Tammann–Fulcher (**VTF**) equation.[7] This nature is followed by graph in Figure S1.

$$\eta = \eta_0 \, exp\left(\frac{B}{(T - T_0)}\right)$$

Where η (mPa.s) viscosity of ILs with T (°C) is the relative temperature, η_0 (mPa.s), B (K), and T_0 (K) are constants. This equation shows the temperature dependency of viscosity.

The Newtonian behavior of four ionic liquid tested on Rheometer at 25 °C and open atmosphere. The nature of each IL shown in Figure S2. This ILs shows the constant viscosity over change in shear rate called Newtonian behavior. But halide anion ILs shown some shear thinning behavior. The iodide anion ILs **2** and **3** shows gel type shear thinning behavior.

The viscosity of four ionic liquid on Rheometer was also taken with varying temperature. However, the measurement was carried out in open atmosphere.

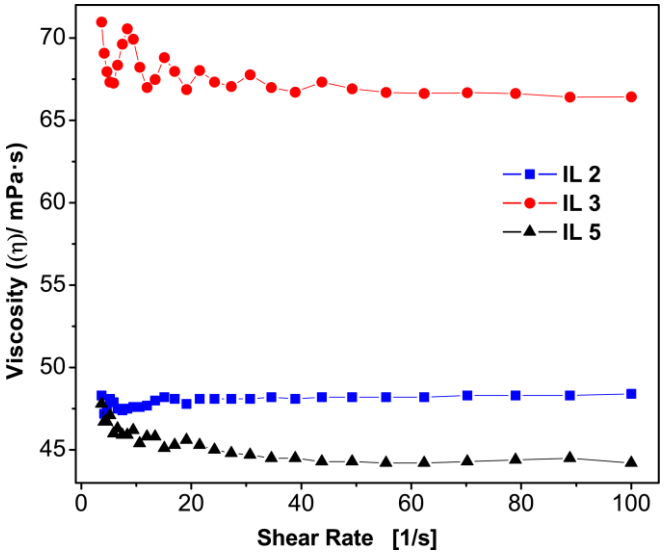

Figure S2. Newtonian behavior of ILs **2**, **3**, **5** at 25 °C.

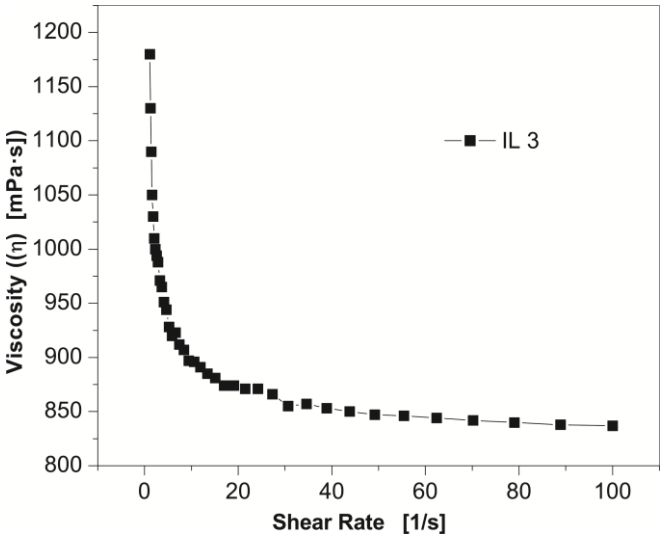

Figure S3. Shear thinning behavior of ILs **3**, at 25 °C.

DSC graphs of Ionic Liquids 1-5:

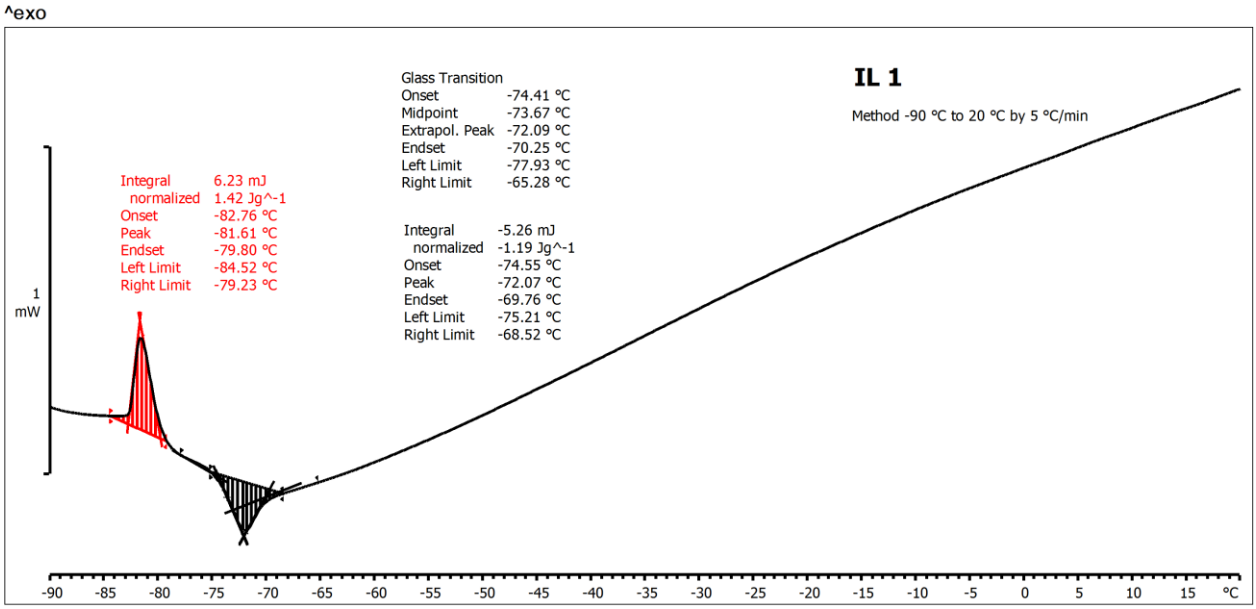

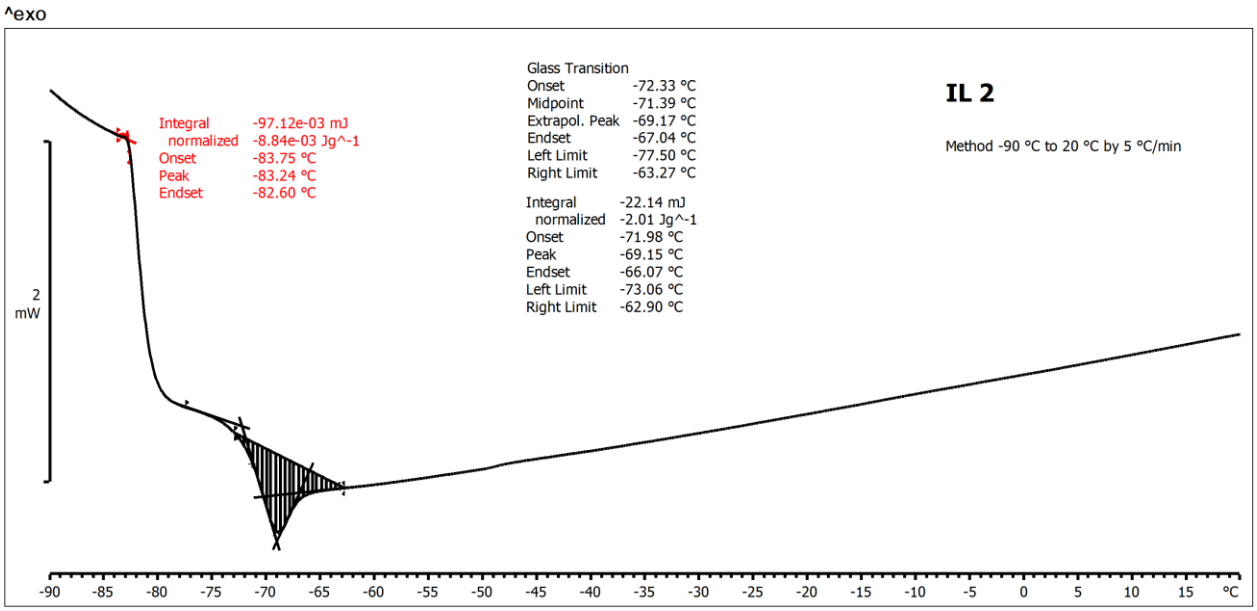
^exo
Integral -97.12e-03 mJ
normalized -8.84e-03 Jg^-1
Onset -83.75 °C
Peak -83.24 °C
Endset -82.60 °C
Glass Transition
Onset -72.33 °C
Midpoint -71.39 °C
Extrapol. Peak -69.17 °C
Endset -67.04 °C
Left Limit -77.50 °C
Right Limit -63.27 °C
Integral -22.14 mJ
normalized -2.01 Jg^-1
Onset -71.98 °C
Peak -69.15 °C
Endset -66.07 °C
Left Limit -73.06 °C
Right Limit -62.90 °C
IL 2
Method -90 °C to 20 °C by 5 °C/min
2
mW
-90 -85 -80 -75 -70 -65 -60 -55 -50 -45 -40 -35 -30 -25 -20 -15 -10 -5 0 5 10 15 °C

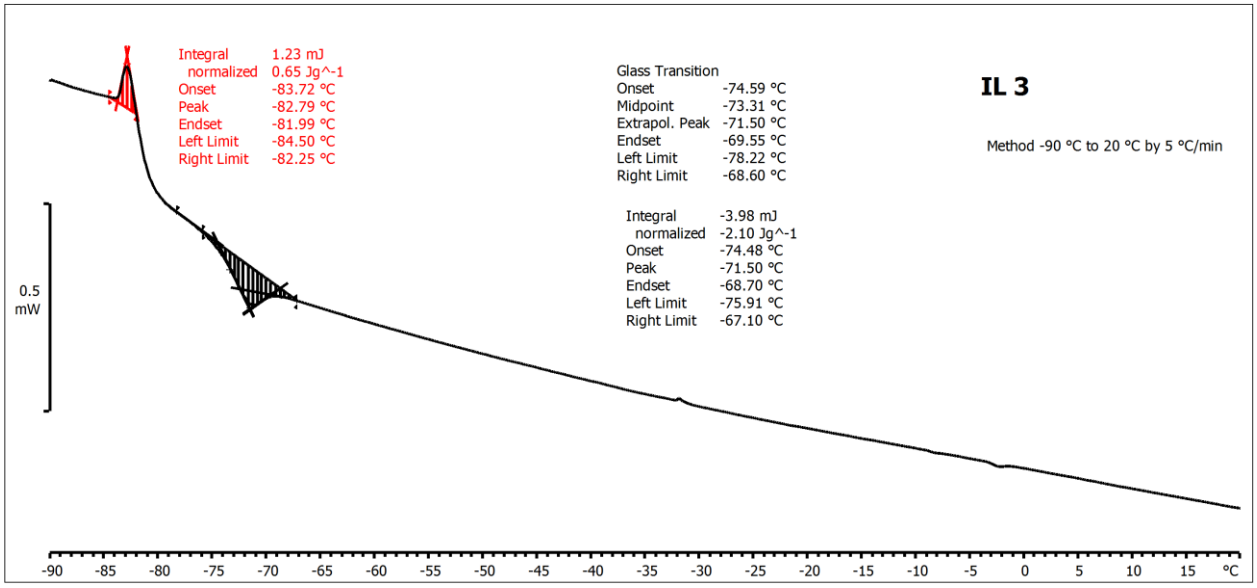
^exo
Integral 1.23 mJ
normalized 0.65 Jg^-1
Onset -83.72 °C
Peak -82.79 °C
Endset -81.99 °C
Left Limit -84.50 °C
Right Limit -82.25 °C
Glass Transition
Onset -74.59 °C
Midpoint -73.31 °C
Extrapol. Peak -71.50 °C
Endset -69.55 °C
Left Limit -78.22 °C
Right Limit -68.60 °C
Integral -3.98 mJ
normalized -2.10 Jg^-1
Onset -74.48 °C
Peak -71.50 °C
Endset -68.70 °C
Left Limit -75.91 °C
Right Limit -67.10 °C
IL 3
Method -90 °C to 20 °C by 5 °C/min
0.5
mW
-90 -85 -80 -75 -70 -65 -60 -55 -50 -45 -40 -35 -30 -25 -20 -15 -10 -5 0 5 10 15 °C

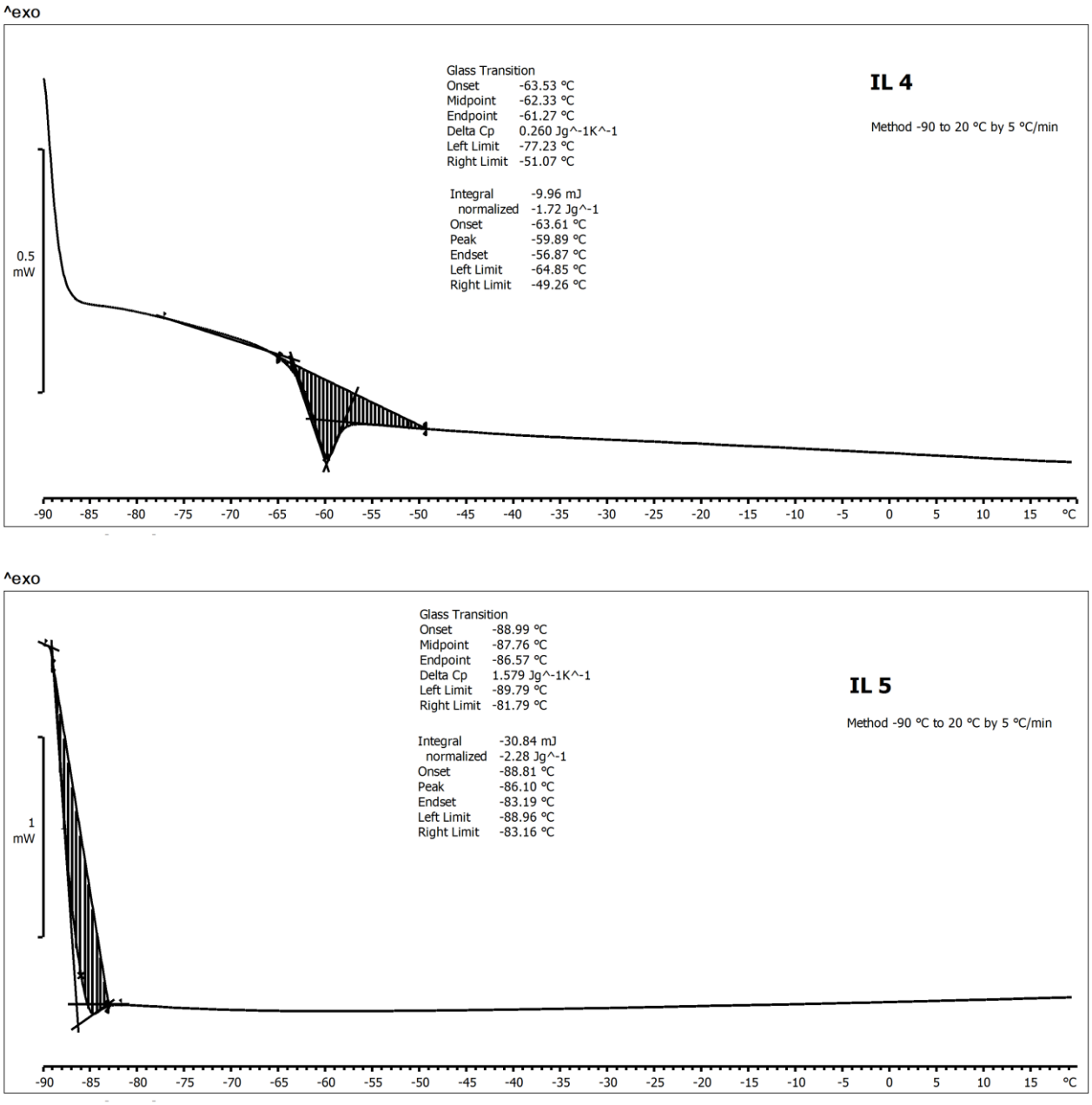

Figure S4. The DSC graphs along with phase transition of ILs **1-5**.

TOPEM Graphs: The reversing signal contains heat capacity related events such as the glass transition. The non-reversing signal contains kinetic events such as crystallization, crystal perfection and reorganization, cure, and decomposition.

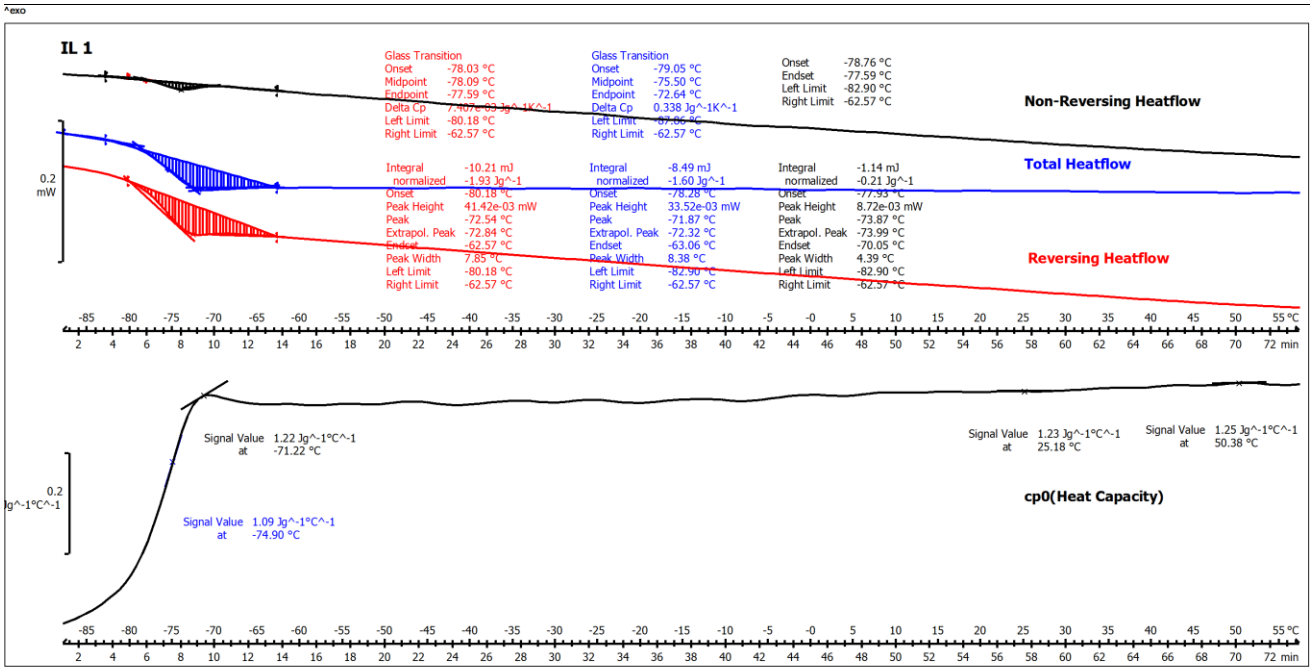

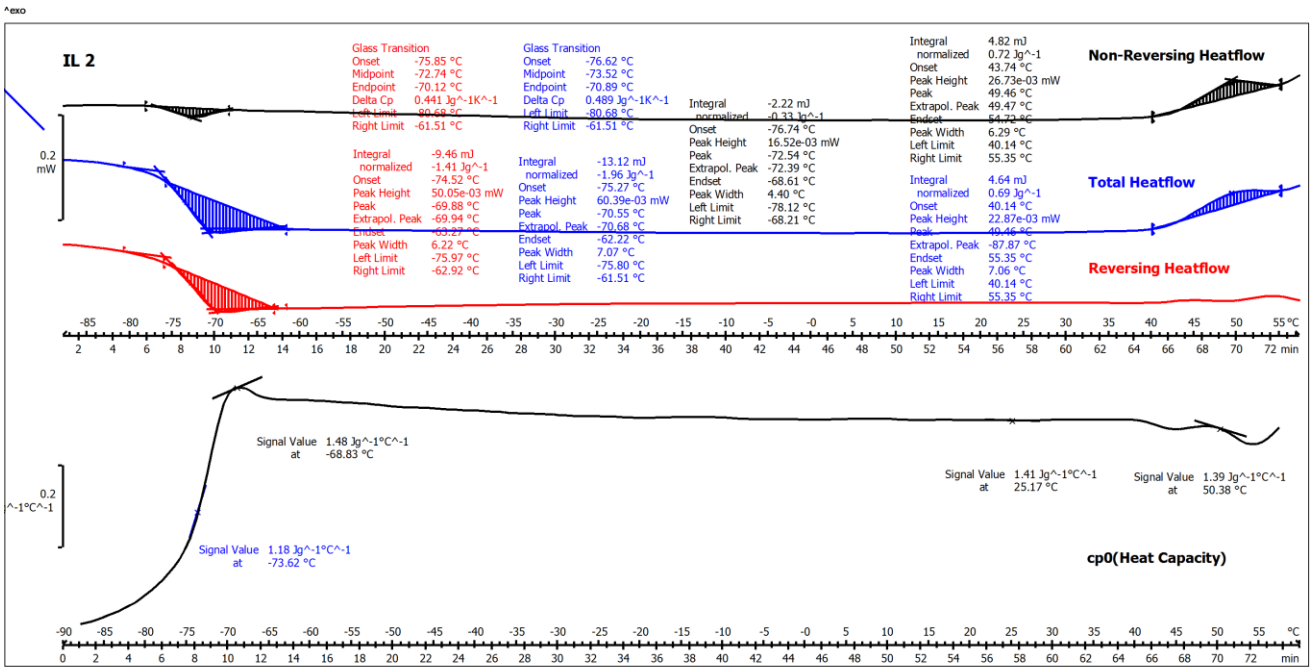

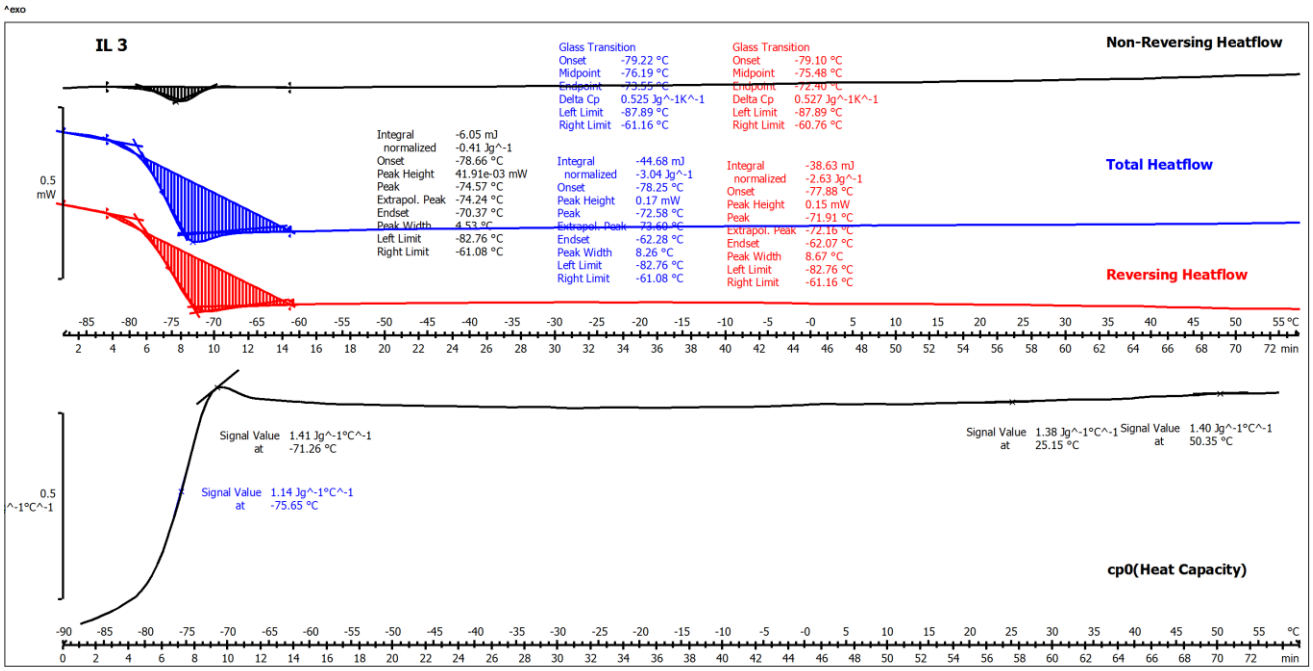
^exo
IL 3
Non-Reversing Heatflow
Glass Transition
Onset -79.22 °C
Midpoint -76.19 °C
Endpoint -73.55 °C
Delta Cp 0.525 Jg^-1K^-1
Left Limit -87.89 °C
Right Limit -61.16 °C
Glass Transition
Onset -79.10 °C
Midpoint -75.48 °C
Endpoint -72.40 °C
Delta Cp 0.527 Jg^-1K^-1
Left Limit -87.89 °C
Right Limit -60.76 °C
Integral -6.05 mJ
normalized -0.41 Jg^-1
Onset -78.66 °C
Peak Height 41.91e-03 mW
Peak -74.57 °C
Extrapol. Peak -74.24 °C
Endset -70.37 °C
Peak Width 4.53 °C
Left Limit -82.76 °C
Right Limit -61.08 °C
Integral -44.68 mJ
normalized -3.04 Jg^-1
Onset -78.25 °C
Peak Height 0.17 mW
Peak -72.58 °C
Extrapol. Peak -73.60 °C
Endset -62.28 °C
Peak Width 8.26 °C
Left Limit -82.76 °C
Right Limit -61.08 °C
Integral -38.63 mJ
normalized -2.63 Jg^-1
Onset -77.88 °C
Peak Height 0.15 mW
Peak -71.91 °C
Extrapol. Peak -72.16 °C
Endset -62.07 °C
Peak Width 8.67 °C
Left Limit -82.76 °C
Right Limit -61.16 °C
Total Heatflow
Reversing Heatflow
0.5 mW
-85 -80 -75 -70 -65 -60 -55 -50 -45 -40 -35 -30 -25 -20 -15 -10 -5 -0 5 10 15 20 25 30 35 40 45 50 55 °C
2 4 6 8 10 12 14 16 18 20 22 24 26 28 30 32 34 36 38 40 42 44 46 48 50 52 54 56 58 60 62 64 66 68 70 72 min
Signal Value 1.41 Jg^-1°C^-1 at -71.26 °C
Signal Value 1.14 Jg^-1°C^-1 at -75.65 °C
Signal Value 1.38 Jg^-1°C^-1 at 25.15 °C
Signal Value 1.40 Jg^-1°C^-1 at 50.35 °C
0.5 ^-1°C^-1
cp0(Heat Capacity)
-90 -85 -80 -75 -70 -65 -60 -55 -50 -45 -40 -35 -30 -25 -20 -15 -10 -5 -0 5 10 15 20 25 30 35 40 45 50 55 °C
0 2 4 6 8 10 12 14 16 18 20 22 24 26 28 30 32 34 36 38 40 42 44 46 48 50 52 54 56 58 60 62 64 66 68 70 72 min

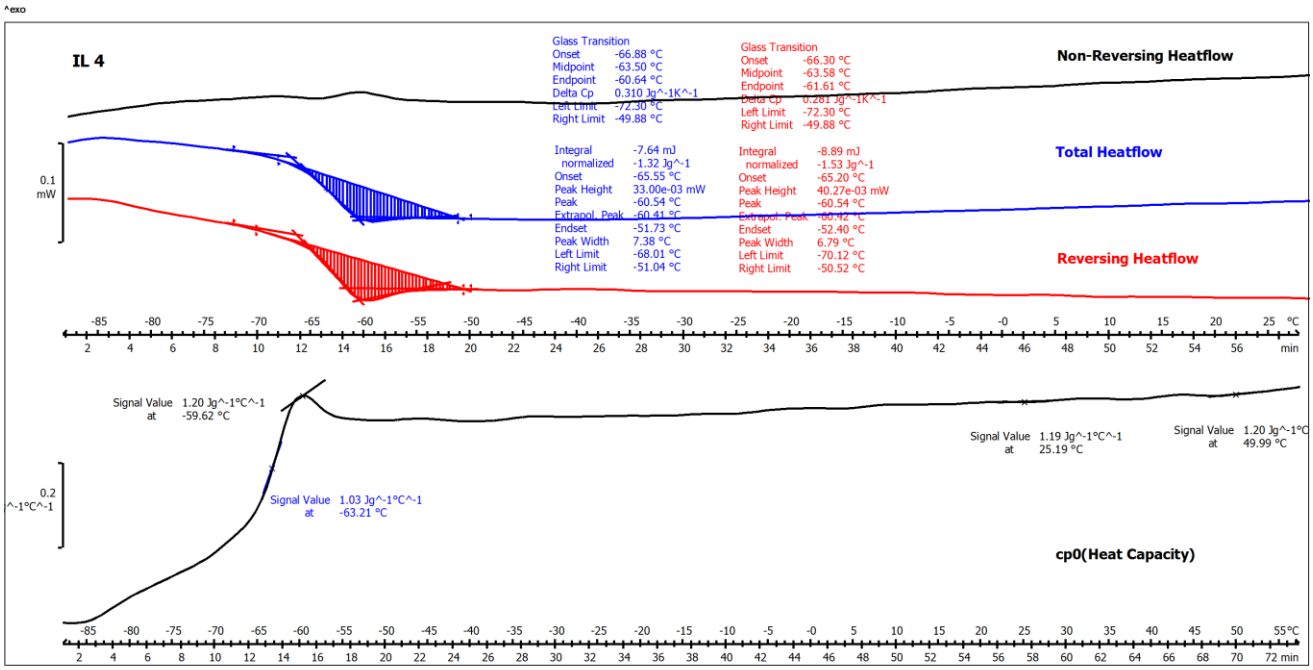
^exo
IL 4
Non-Reversing Heatflow
Glass Transition
Onset -66.88 °C
Midpoint -63.50 °C
Endpoint -60.64 °C
Delta Cp 0.310 Jg^-1K^-1
Left Limit -72.30 °C
Right Limit -49.88 °C
Glass Transition
Onset -66.30 °C
Midpoint -63.58 °C
Endpoint -61.61 °C
Delta Cp 0.281 Jg^-1K^-1
Left Limit -72.30 °C
Right Limit -49.88 °C
Integral -7.64 mJ
normalized -1.32 Jg^-1
Onset -65.55 °C
Peak Height 33.00e-03 mW
Peak -60.54 °C
Extrapol. Peak -60.41 °C
Endset -51.73 °C
Peak Width 7.38 °C
Left Limit -68.01 °C
Right Limit -51.04 °C
Integral -8.89 mJ
normalized -1.53 Jg^-1
Onset -65.20 °C
Peak Height 40.27e-03 mW
Peak -60.54 °C
Extrapol. Peak -60.42 °C
Endset -52.40 °C
Peak Width 6.79 °C
Left Limit -70.12 °C
Right Limit -50.52 °C
Total Heatflow
Reversing Heatflow
0.1 mW
-85 -80 -75 -70 -65 -60 -55 -50 -45 -40 -35 -30 -25 -20 -15 -10 -5 -0 5 10 15 20 25 °C
2 4 6 8 10 12 14 16 18 20 22 24 26 28 30 32 34 36 38 40 42 44 46 48 50 52 54 56 min
Signal Value 1.20 Jg^-1°C^-1 at -59.62 °C
Signal Value 1.03 Jg^-1°C^-1 at -63.21 °C
Signal Value 1.19 Jg^-1°C^-1 at 25.19 °C
Signal Value 1.20 Jg^-1°C at 49.99 °C
0.2 ^-1°C^-1
cp0(Heat Capacity)
-85 -80 -75 -70 -65 -60 -55 -50 -45 -40 -35 -30 -25 -20 -15 -10 -5 -0 5 10 15 20 25 30 35 40 45 50 55°C
2 4 6 8 10 12 14 16 18 20 22 24 26 28 30 32 34 36 38 40 42 44 46 48 50 52 54 56 58 60 62 64 66 68 70 72 min

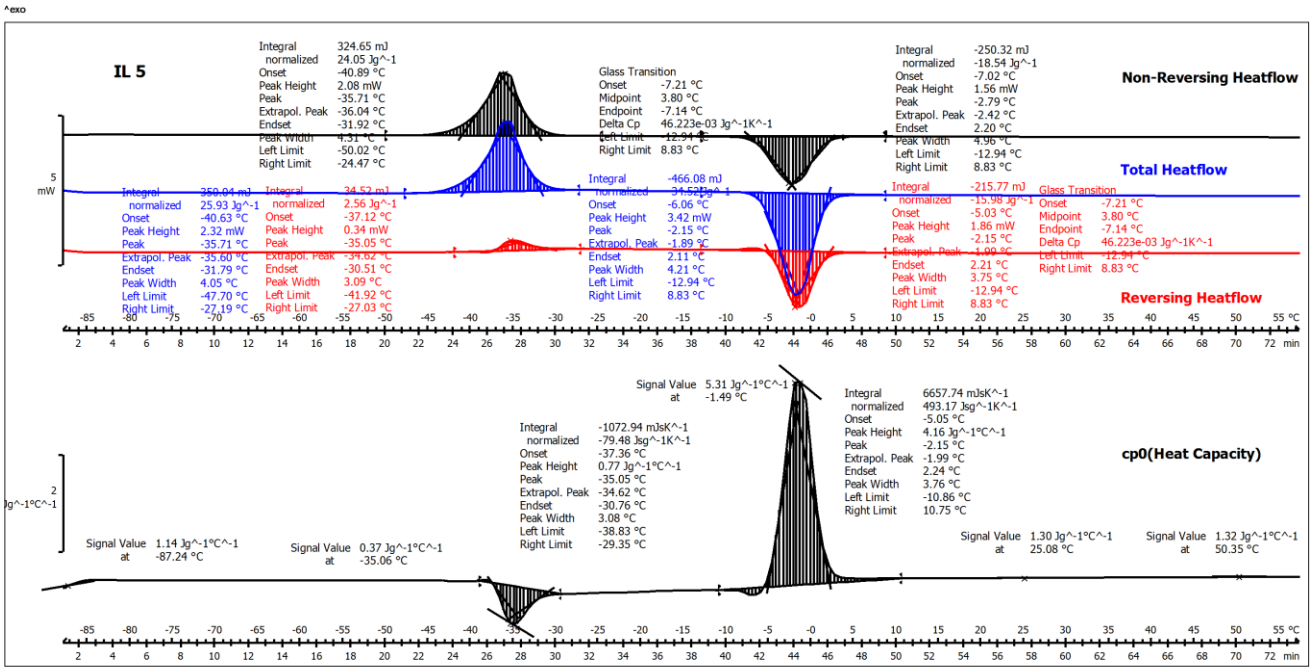

Figure S5. The TOPEM® graph of ILs **1-5**. The heat capacity of ionic liquid, at different temperature from –90 °C to 60 °C heating by 2 °C.min^{-1} and phase transition temperature were confirmed by TOPEM®

Comparison of NMR Data ILs (1-5):

Table S2:

ILs	C2-H Im	NCH2O	NCH2	NCH2SiOSi	NCH2Si	NCH2O	NCH3	F19-TFSI
1O2-Im-1SiOSi (**1**)	8.55	4.33	n	3.74	n	n	n	–78.91
1O2O2-Im-1SiOSi (**2**)	8.71	4.36	n	3.74	n	n	n	–78.19
1O2O2-Im-2O1 (**3**)	8.80	4.41-4.27	n	n	n	3.88-3.79	n	–78.85
Si-Im-2-SiOSi (**4**)	8.65	n	n	3.78	3.84	n	n	–78.77
BMIM (**5**)	8.71	n	4.14	n	n	n	3.91	–79.25

NMR Images:

IL 5a:

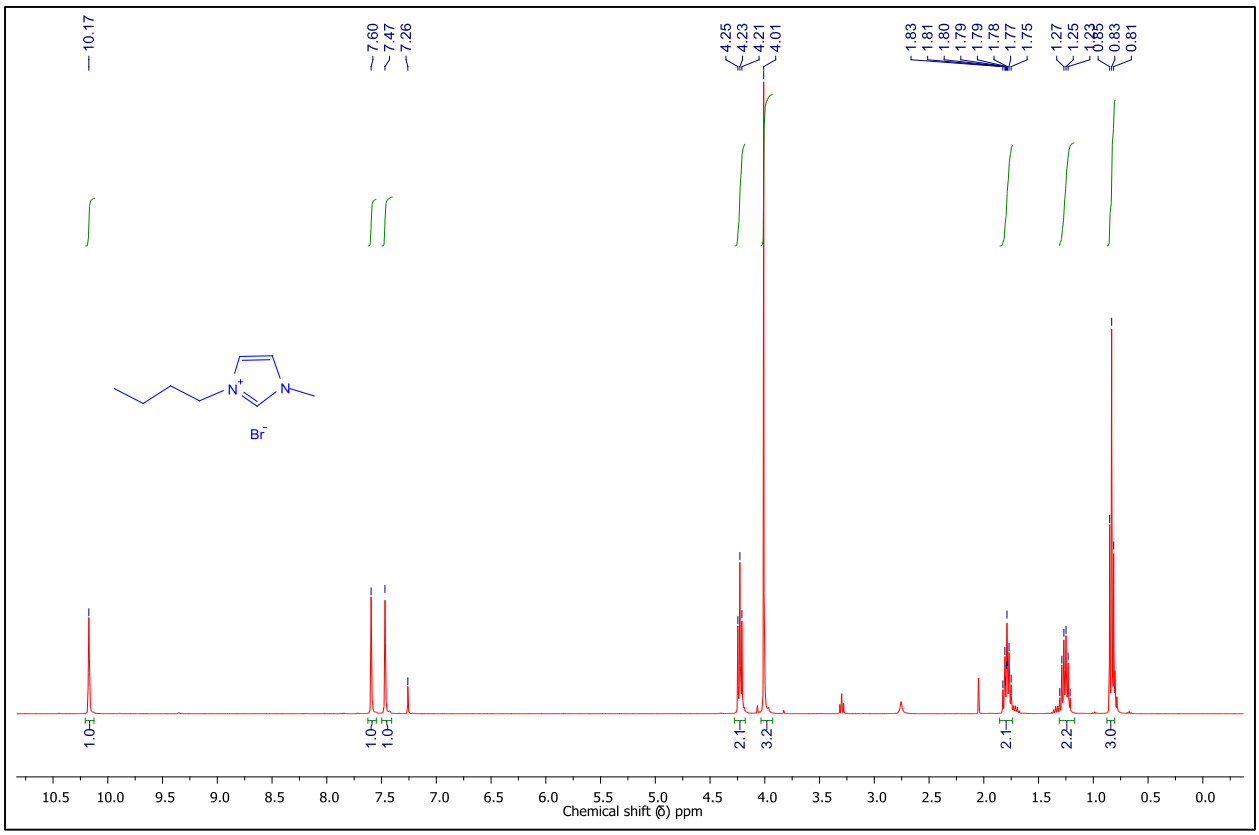

Figure S6: ^{1}H NMR spectrum of compound **5a** in $CDCl_3$ (NMR was taken after 10 min of MW irradiation for monitoring reaction progress; directly from the reaction mixture)

IL 1.

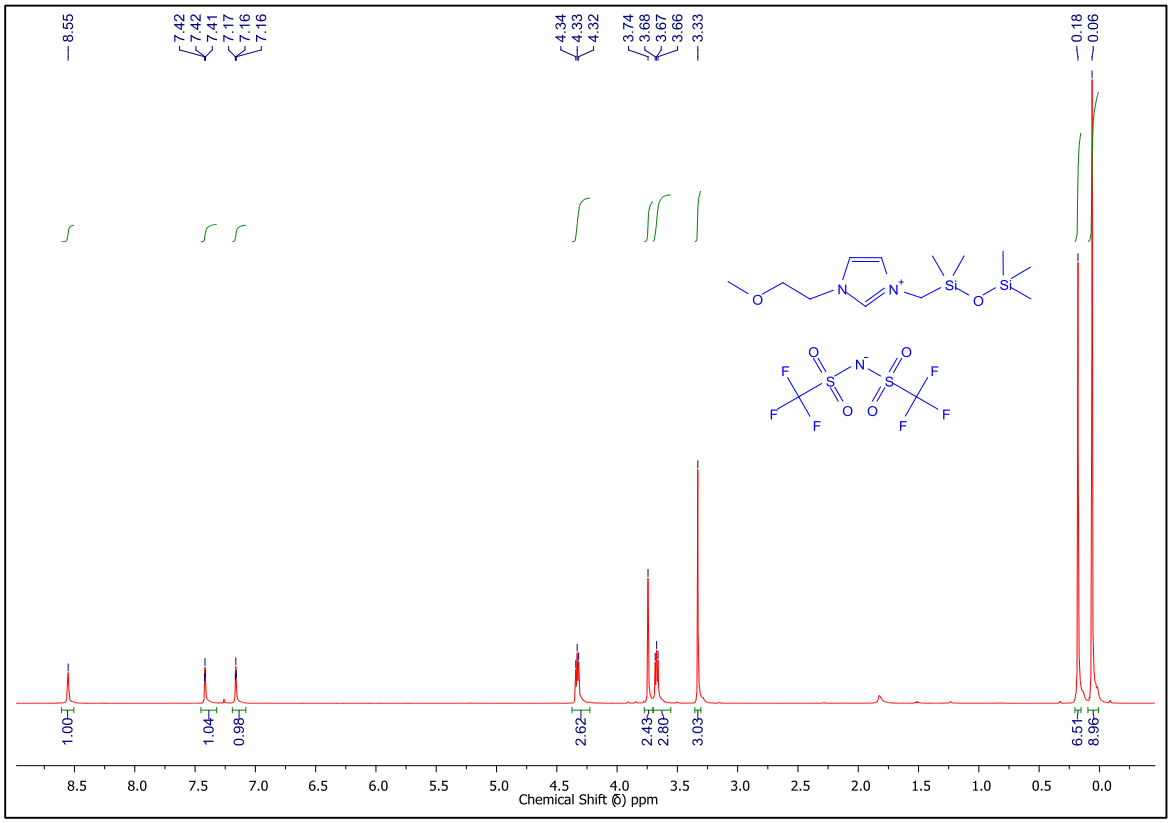

Figure S7: ^{1}H NMR spectrum of IL **1** in $CDCl_3$

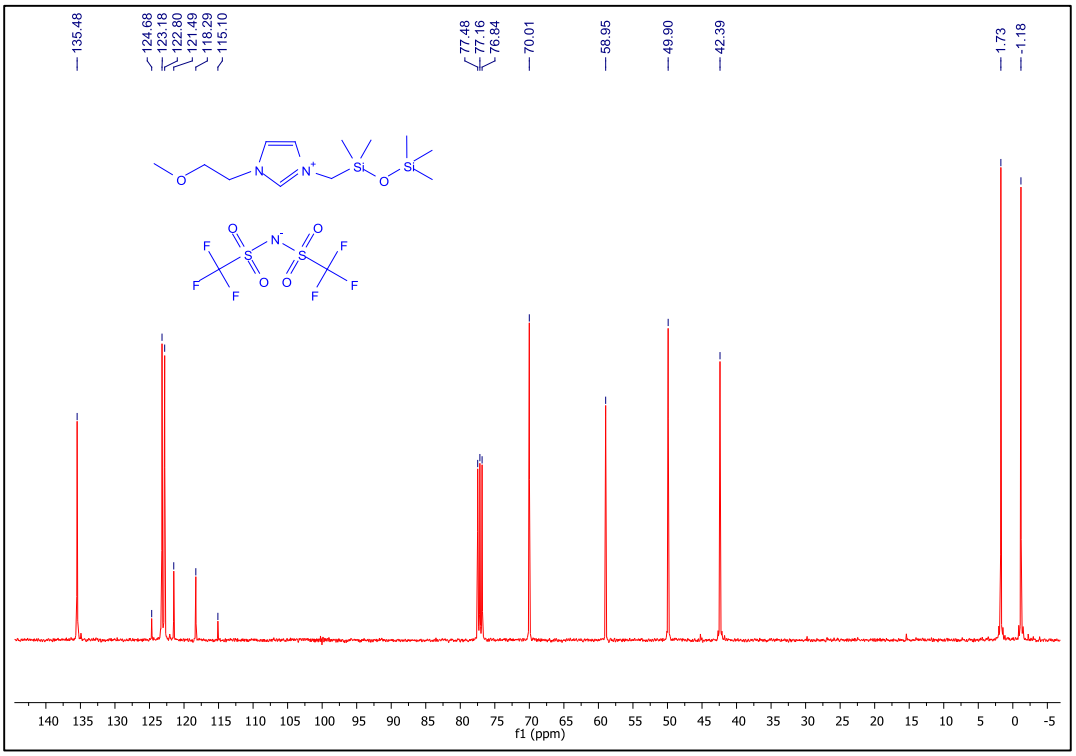

Figure S8: $^{13}C\{^{1}H\}$ NMR spectrum of IL **1** in $CDCl_3$

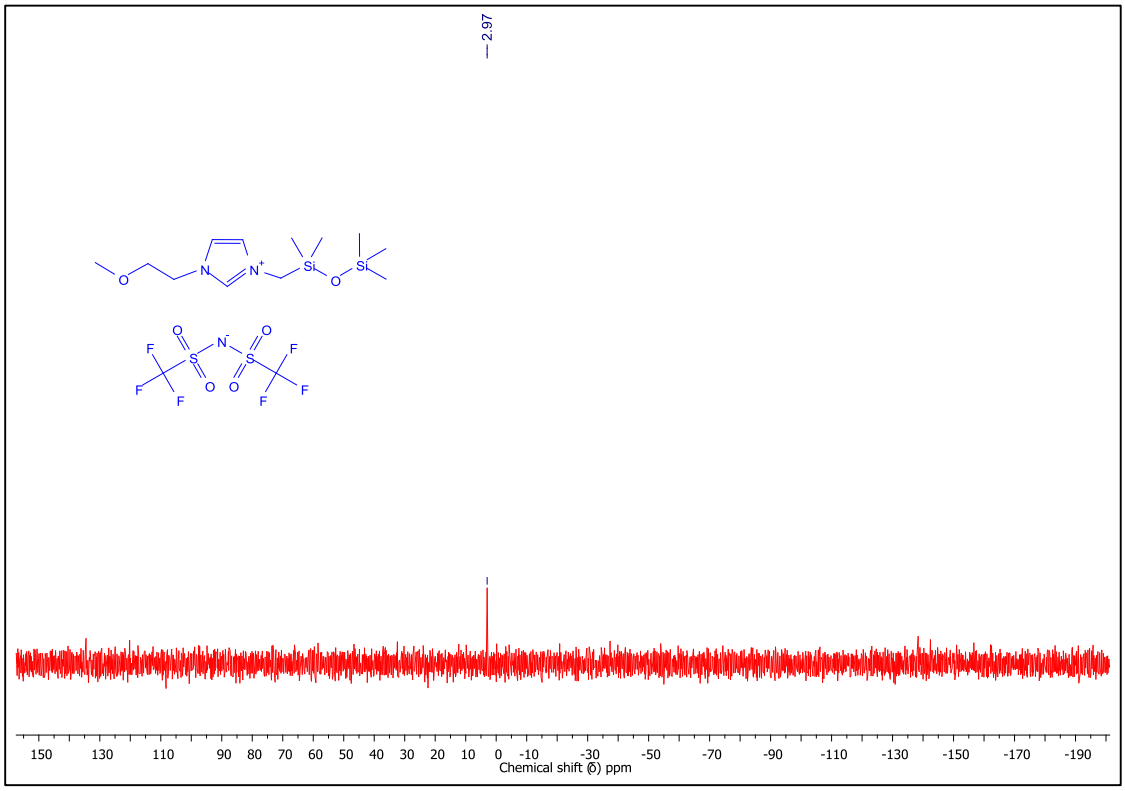

Figure S9: $^{29}Si\{^{1}H\}$ NMR spectrum of IL **1** in $CDCl_3$

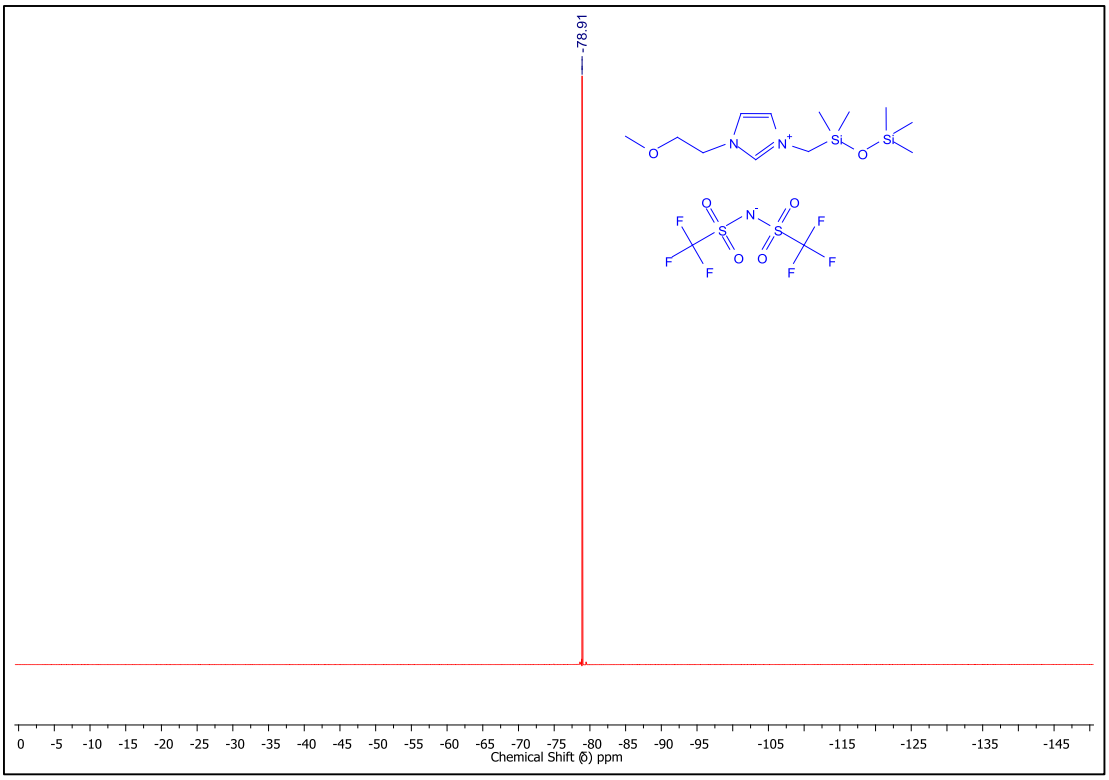

Figure S10: ^{19}F NMR spectrum of IL **1** in $CDCl_3$

IL 2.

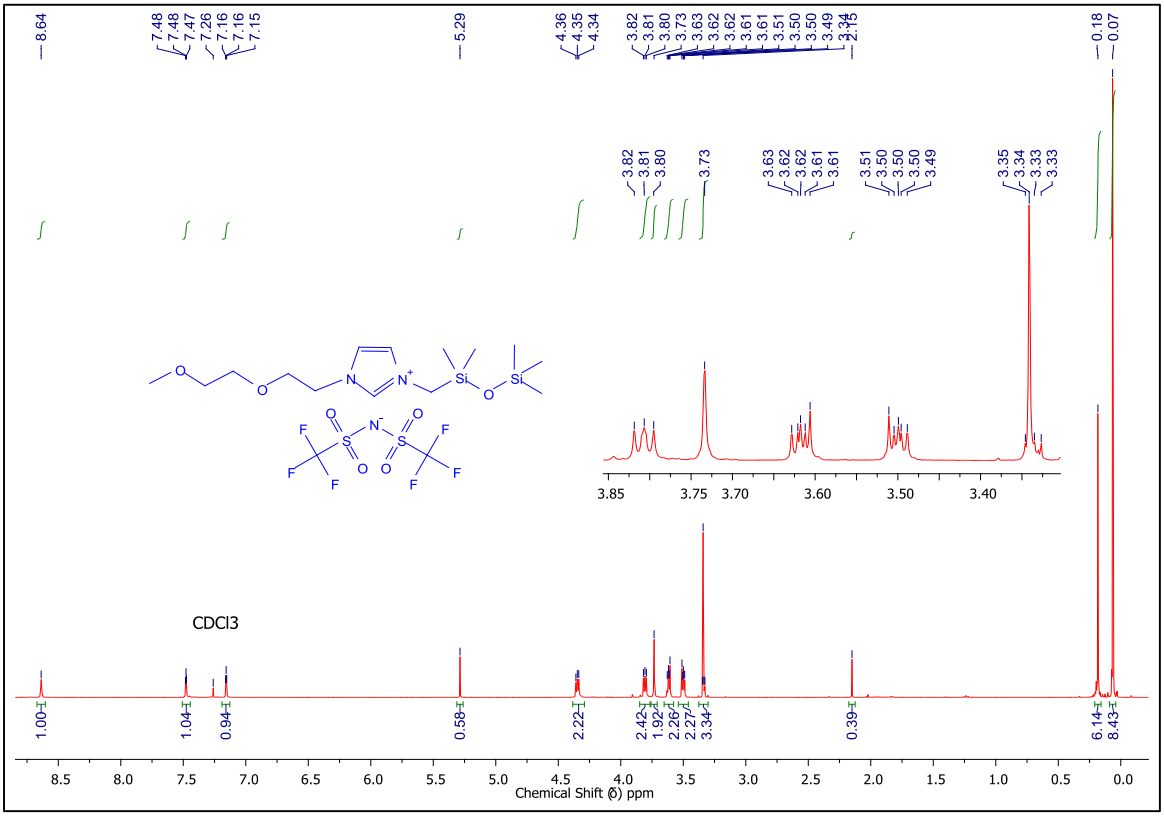

Figure S11: ^{1}H NMR spectrum of IL **2** in $CDCl_3$

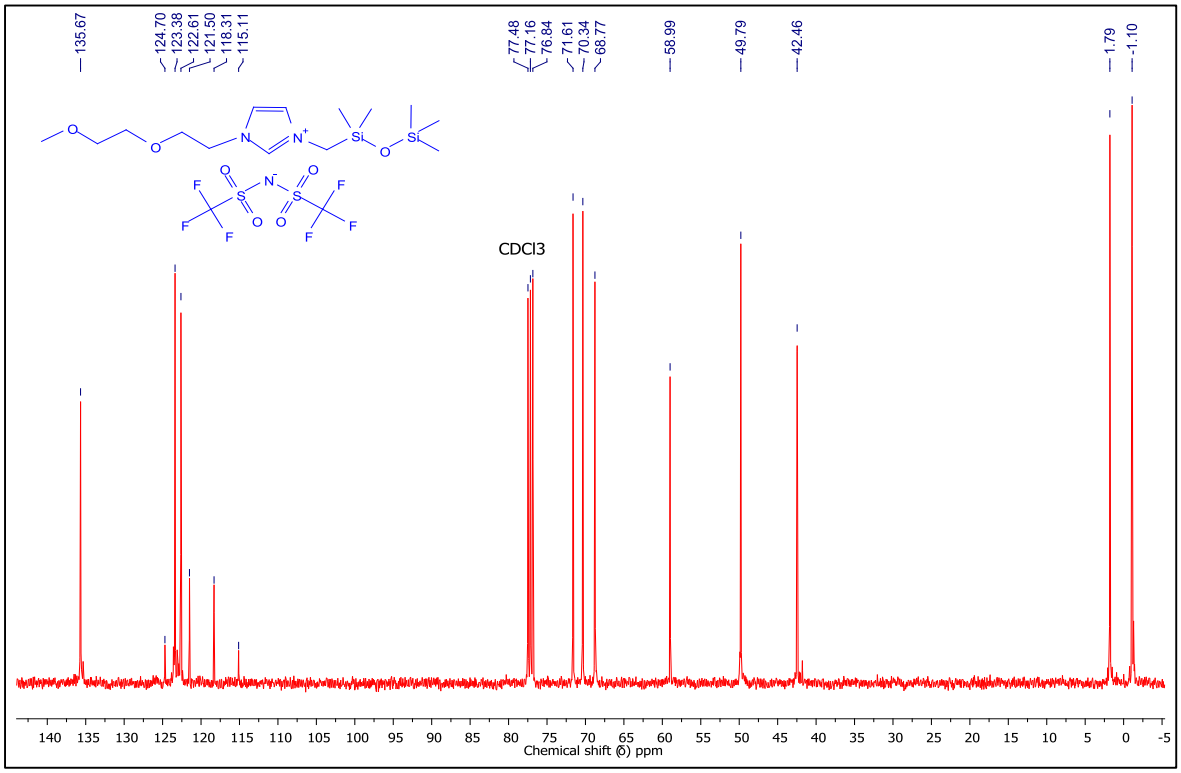

Figure S12: ^{13}C {^{1}H} NMR spectrum of IL **2** in $CDCl_3$

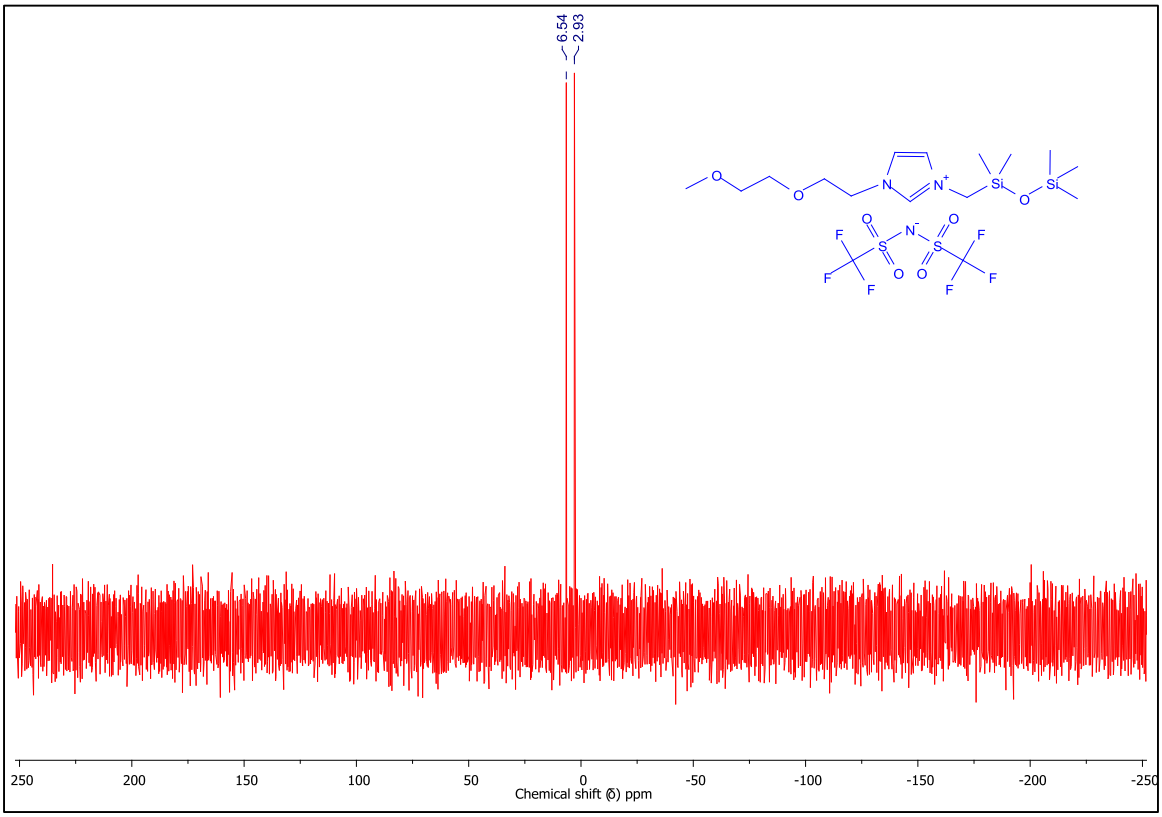

Figure S13: $^{29}Si\{^{1}H\}$ NMR spectrum of IL **2** in $CDCl_3$

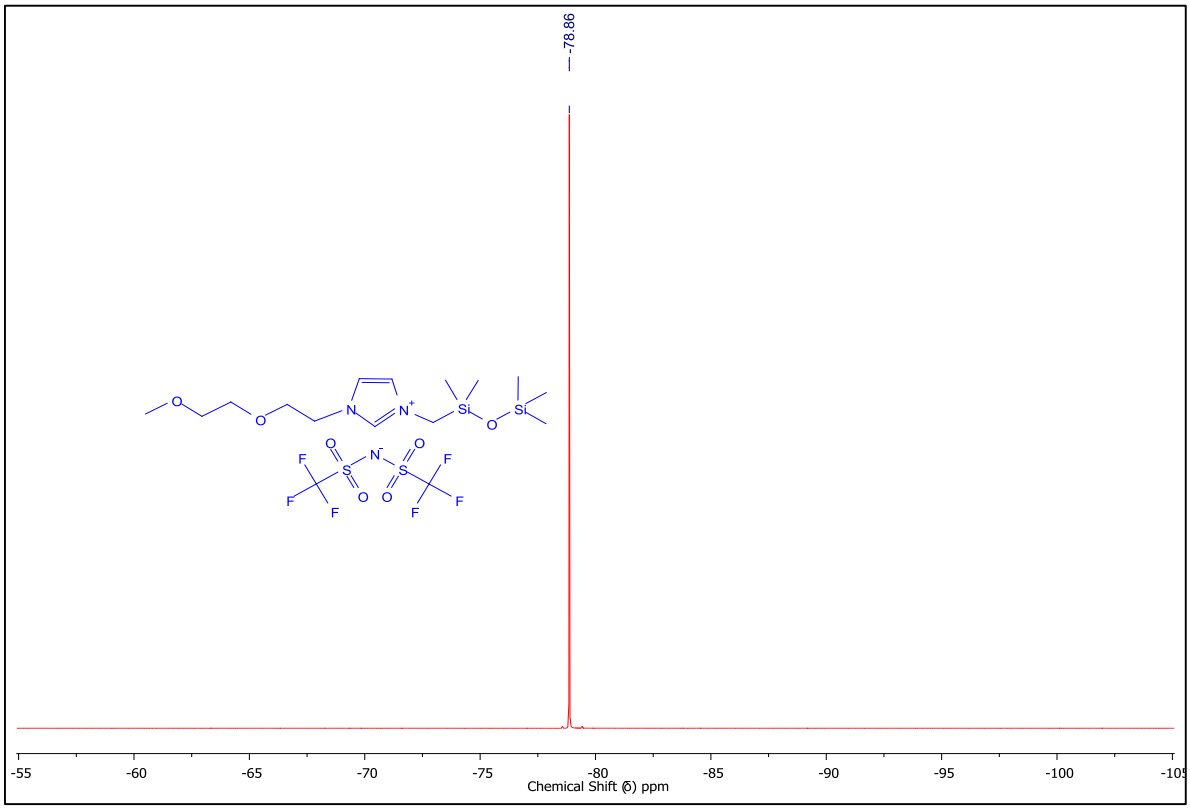

Figure S14: ^{19}F NMR spectrum of IL **2** in $CDCl_3$

IL 3.

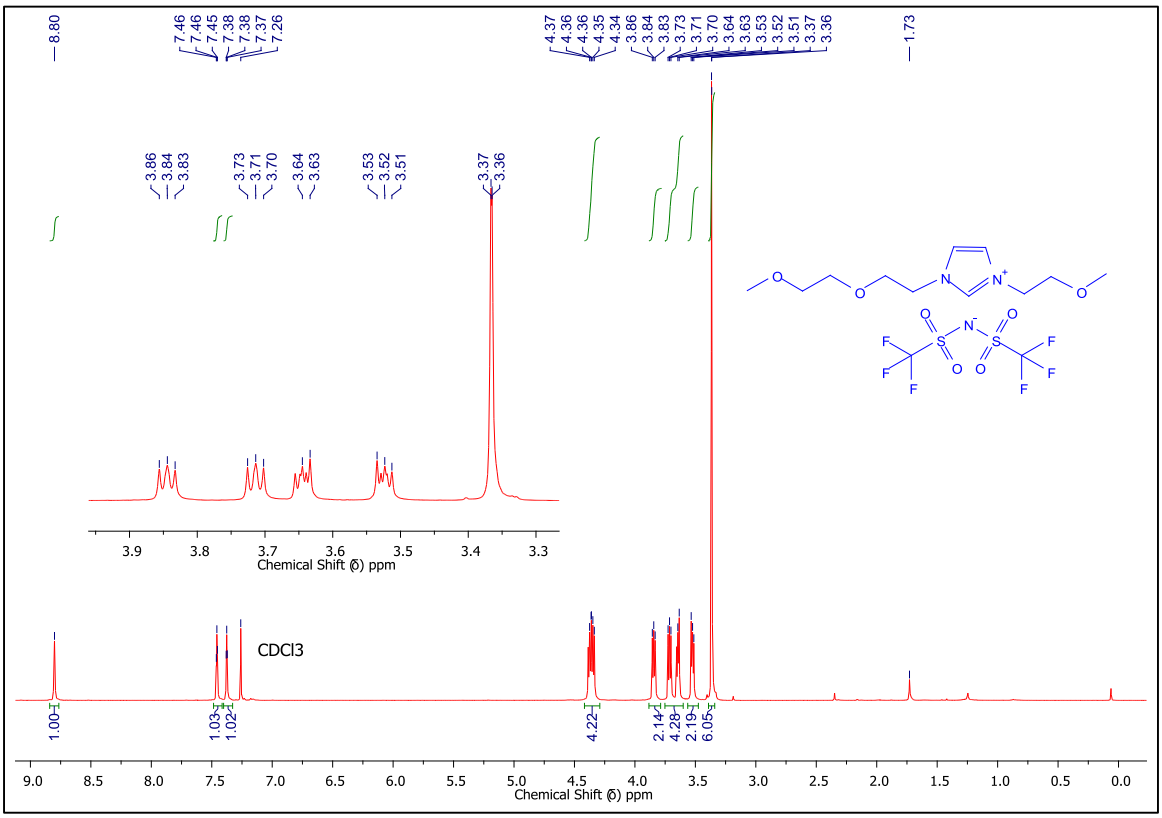

Figure S15: ^{1}H NMR spectrum of IL **3** in $CDCl_3$

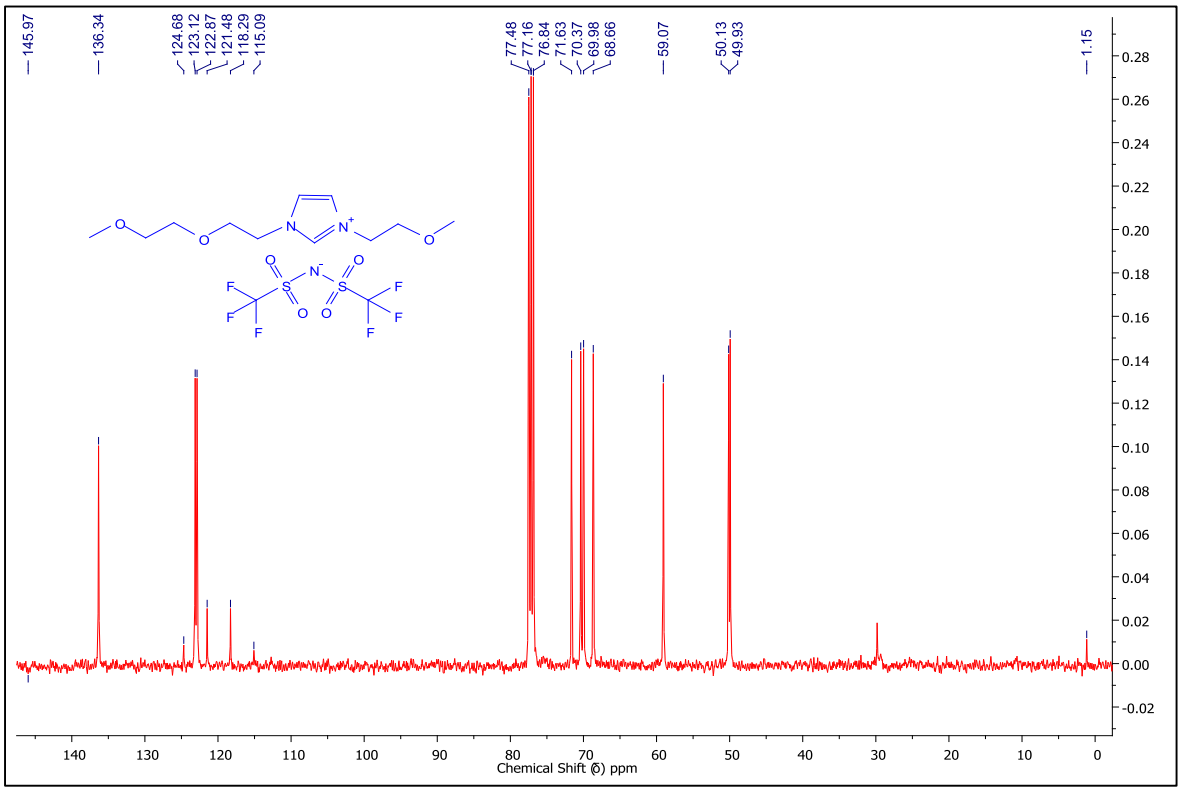

Figure S16: $^{13}C\{^{1}H\}$ NMR spectrum of IL **3** in $CDCl_3$

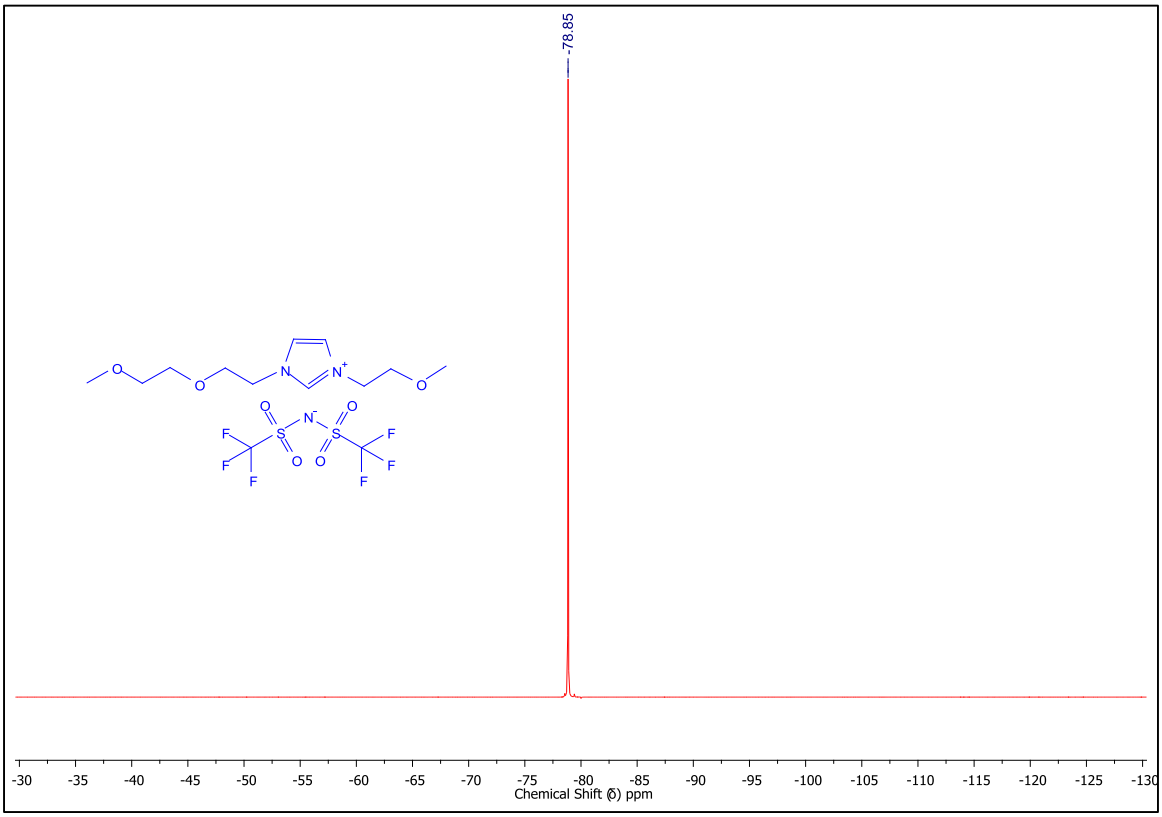

Figure S17: ^{19}F NMR spectrum of IL **3** in $CDCl_3$

IL 4.

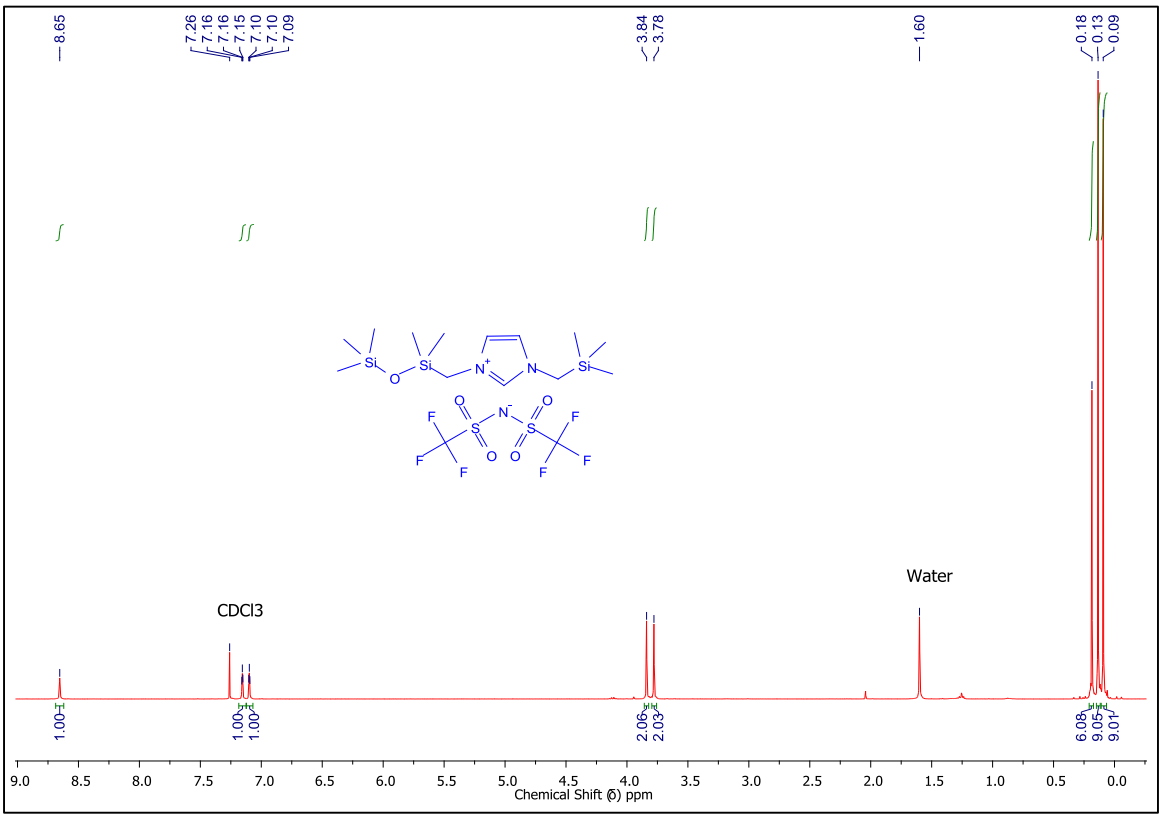

Figure S18: ^{1}H NMR spectrum of IL **4** in $CDCl_3$

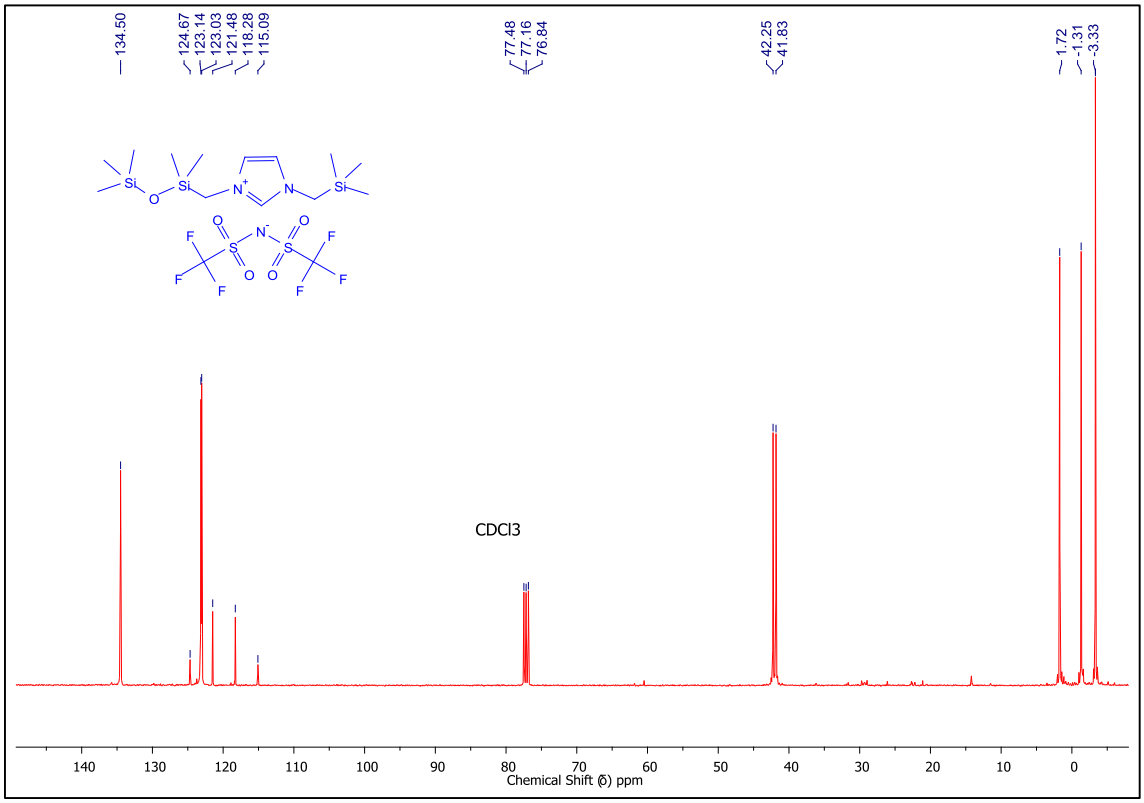

Figure S19: $^{13}C\{^{1}H\}$ NMR spectrum of IL **4** in $CDCl_3$

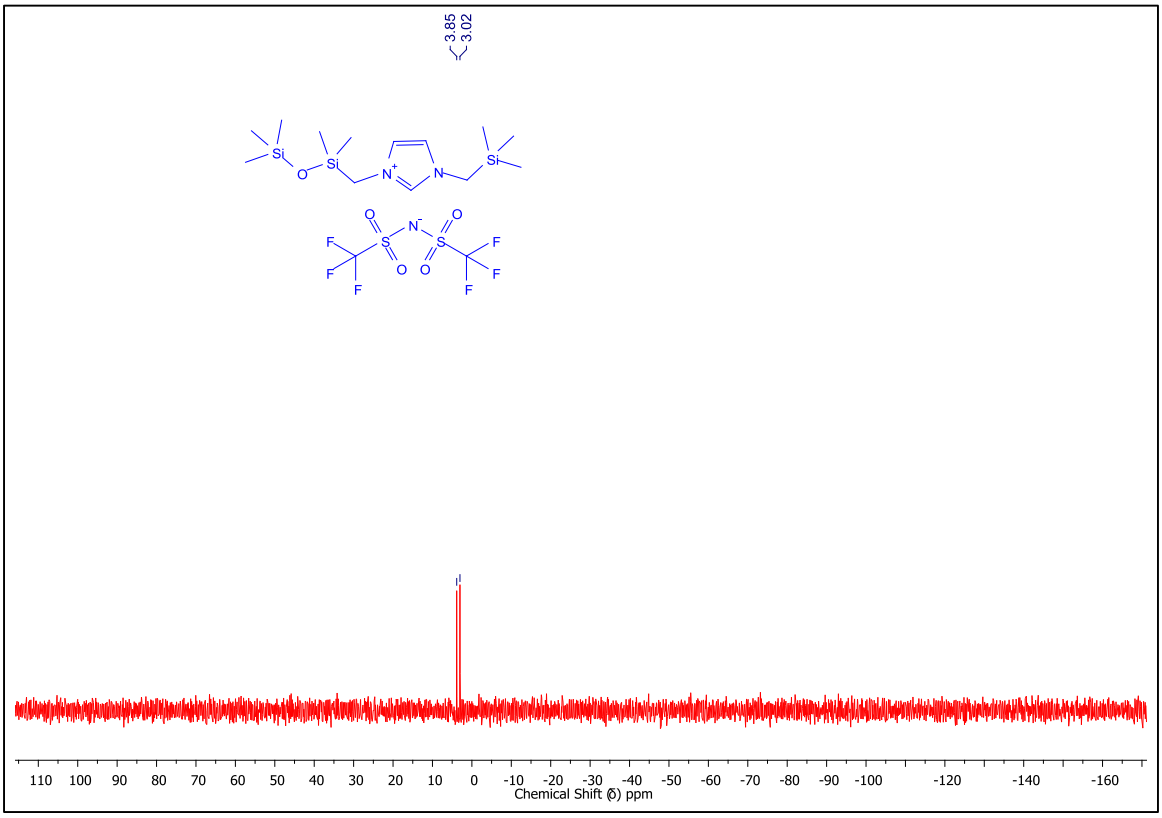

Figure S20: $^{29}Si\{^{1}H\}$ NMR spectrum of IL **4** in $CDCl_3$

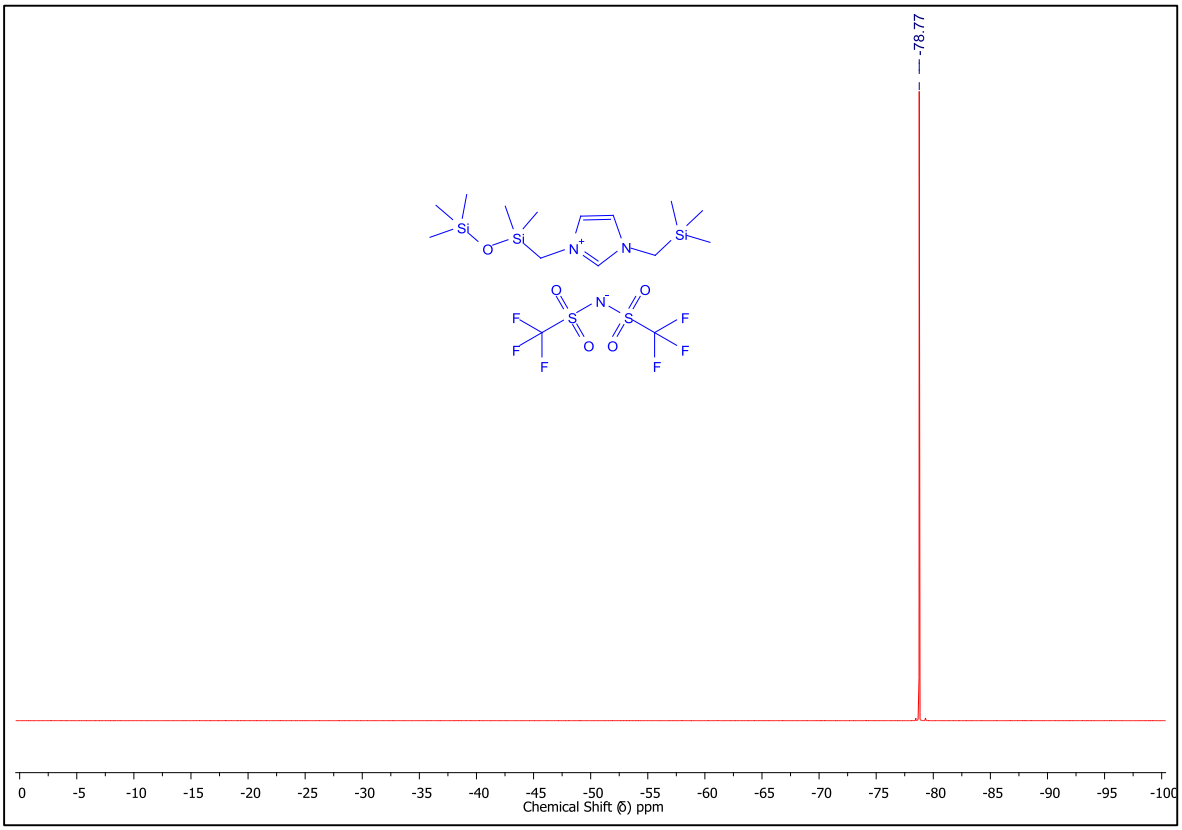

Figure S21: ^{19}F NMR spectrum of IL **4** in $CDCl_3$

IL 5.

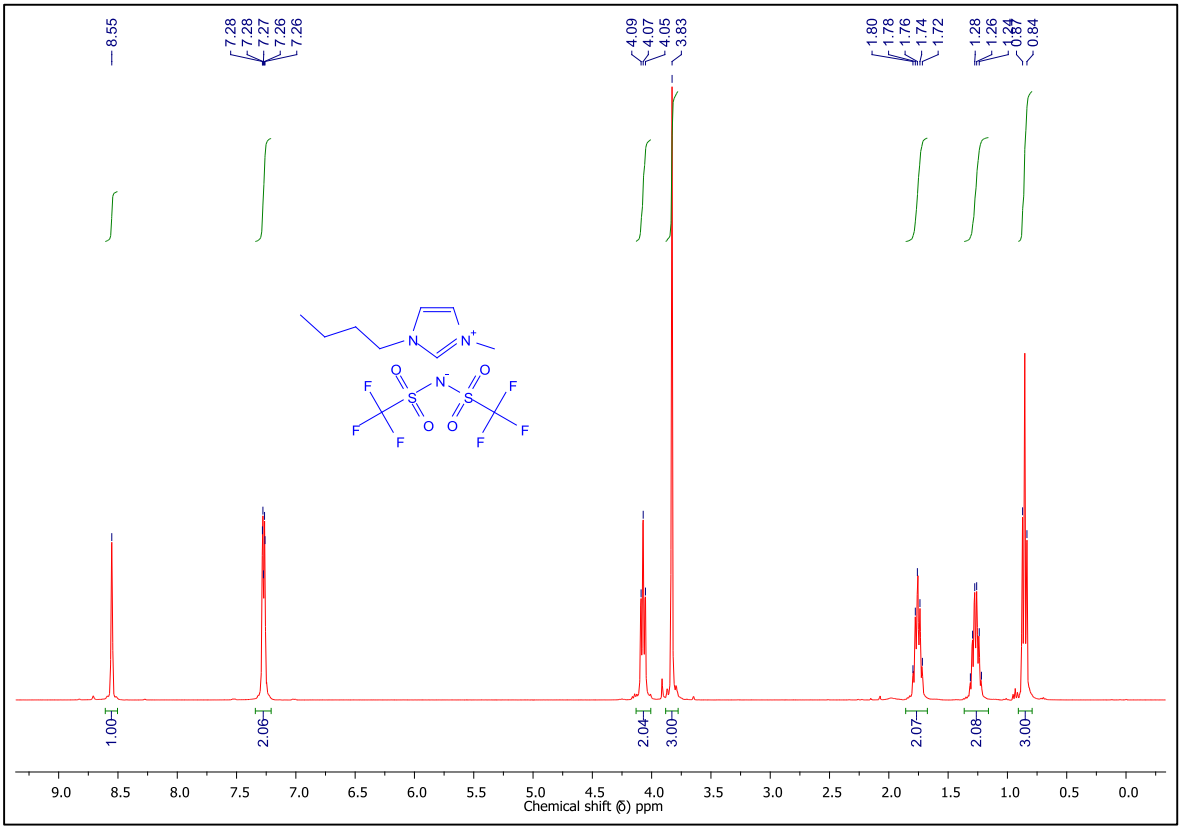

Figure S22: ^{1}H NMR spectrum of IL **5** in $CDCl_3$

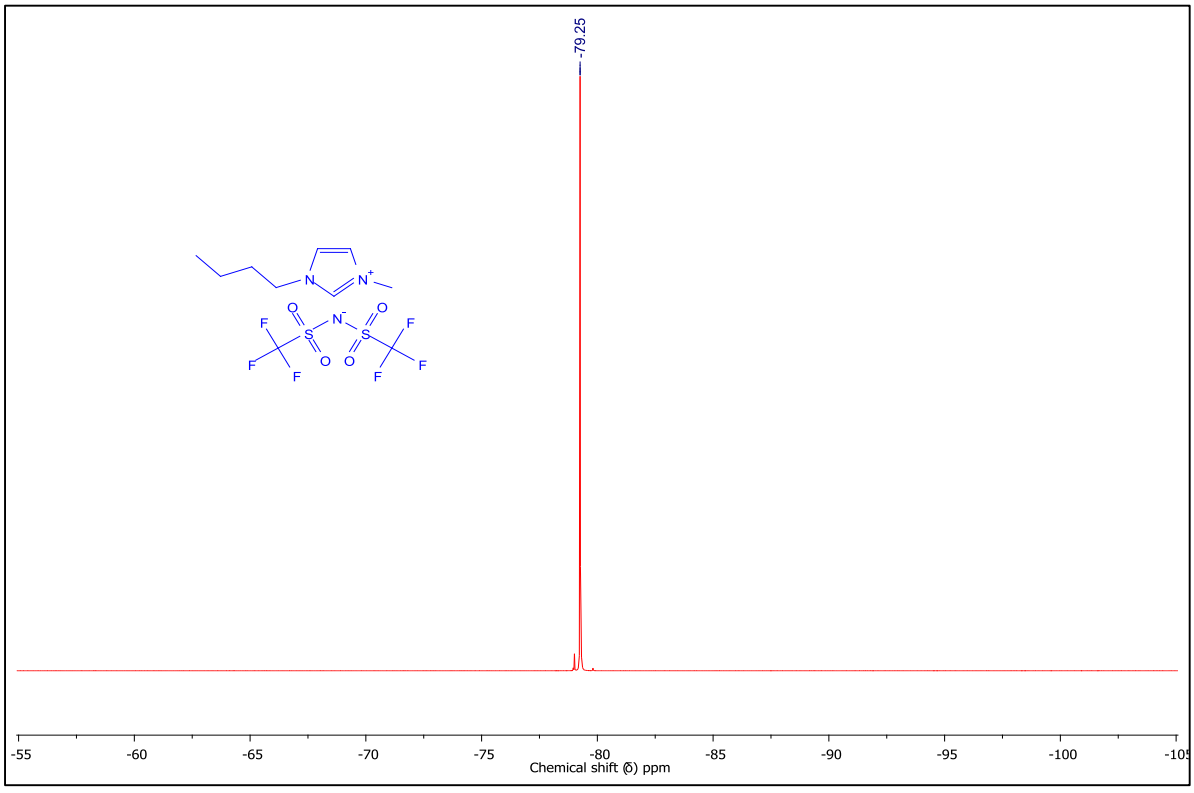

Figure S23: ^{19}F NMR spectrum of compound **5** in $CDCl_3$

Compound 1a

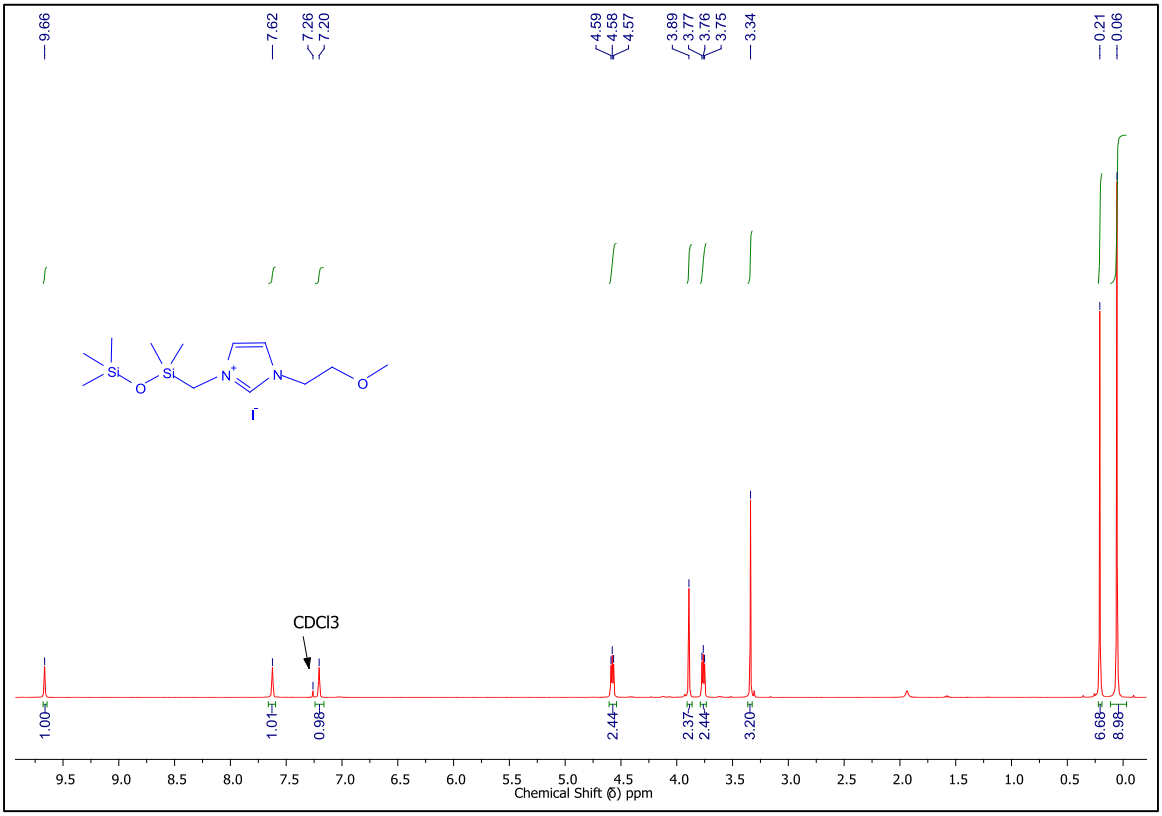

Figure S24: ^{1}H NMR spectrum of compound **1a** in $CDCl_3$

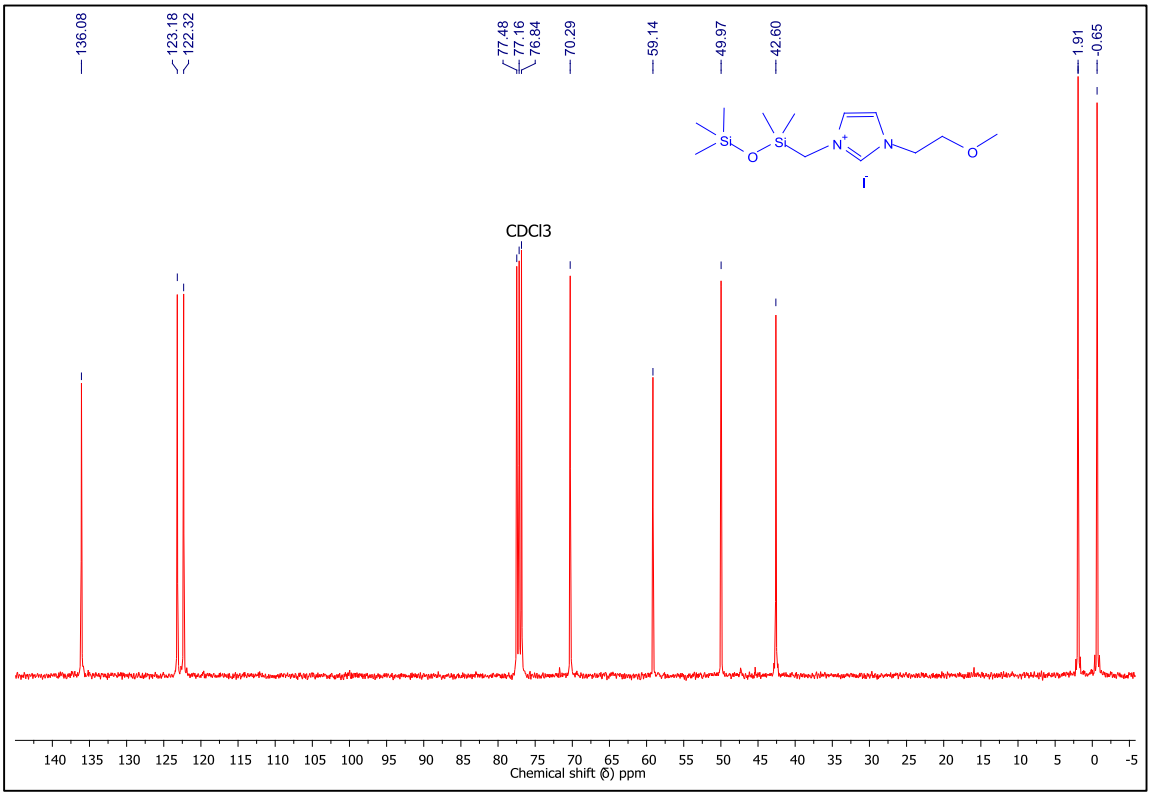

Figure S25: ^{13}C $\{^{1}H\}$ NMR spectrum of compound **1a** in $CDCl_3$

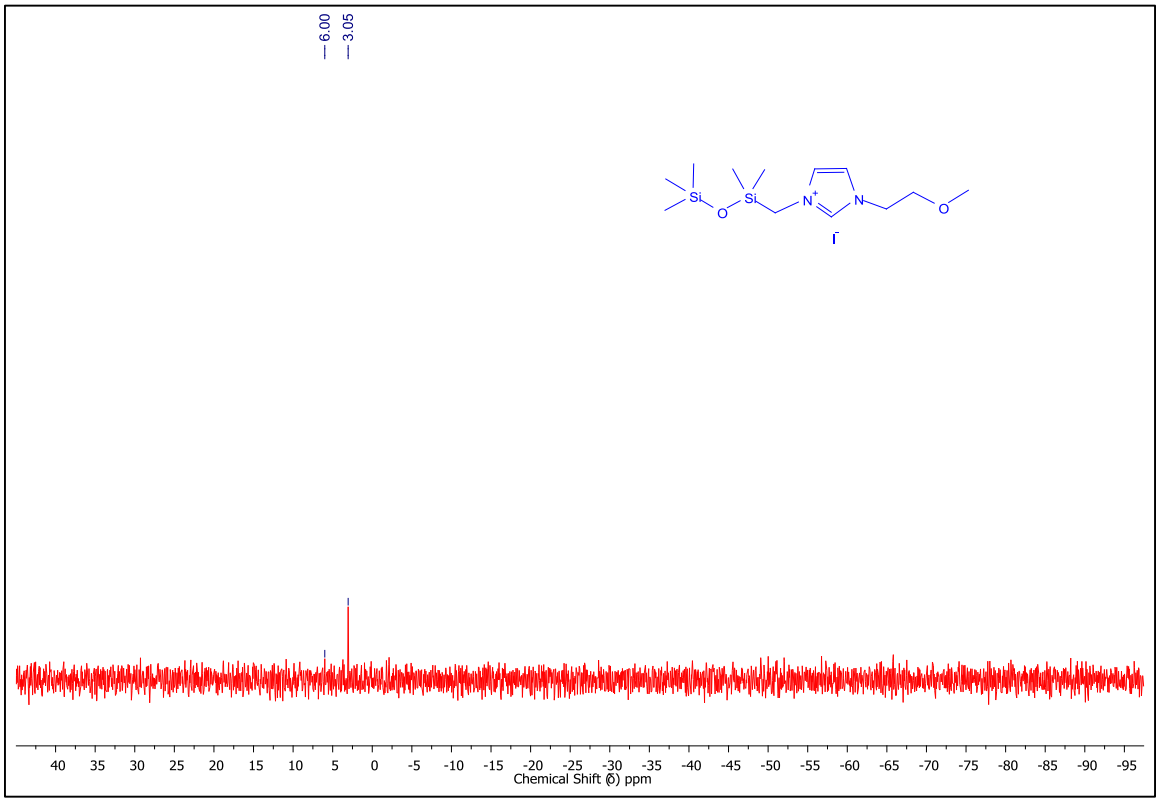

Figure S26: ^{29}Si $\{^{1}H\}$ NMR spectrum of compound **1a** in $CDCl_3$

Compound 2a.

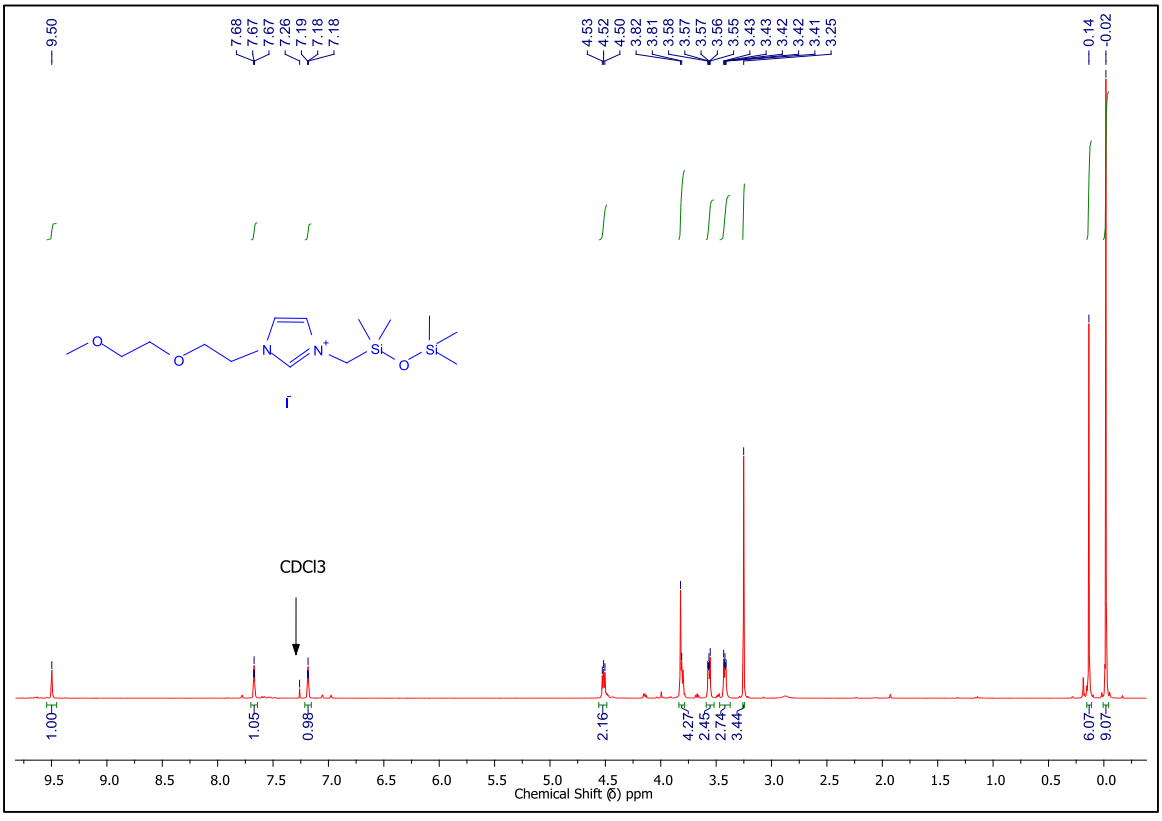

Figure S27: ^{1}H NMR spectrum of compound **2a** in $CDCl_3$

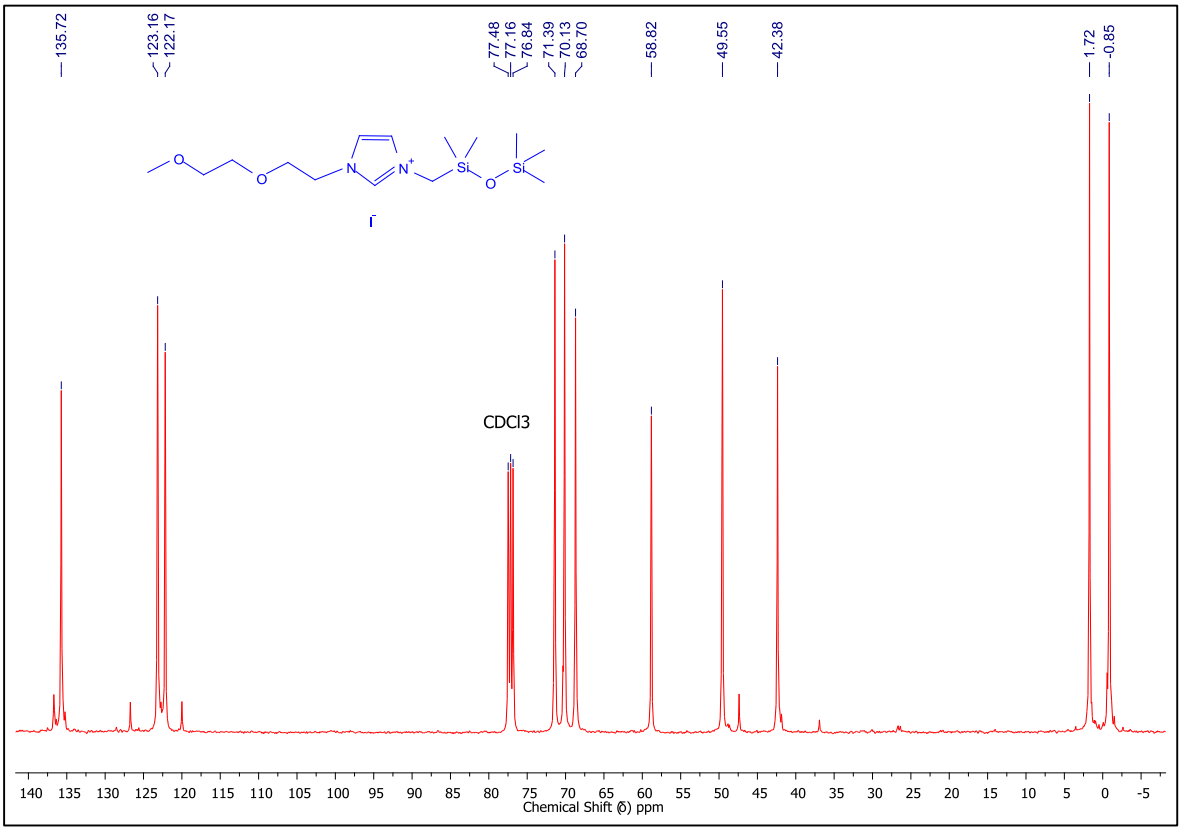

Figure S28: $^{13}C\{^{1}H\}$ NMR spectrum of compound **2a** in $CDCl_3$

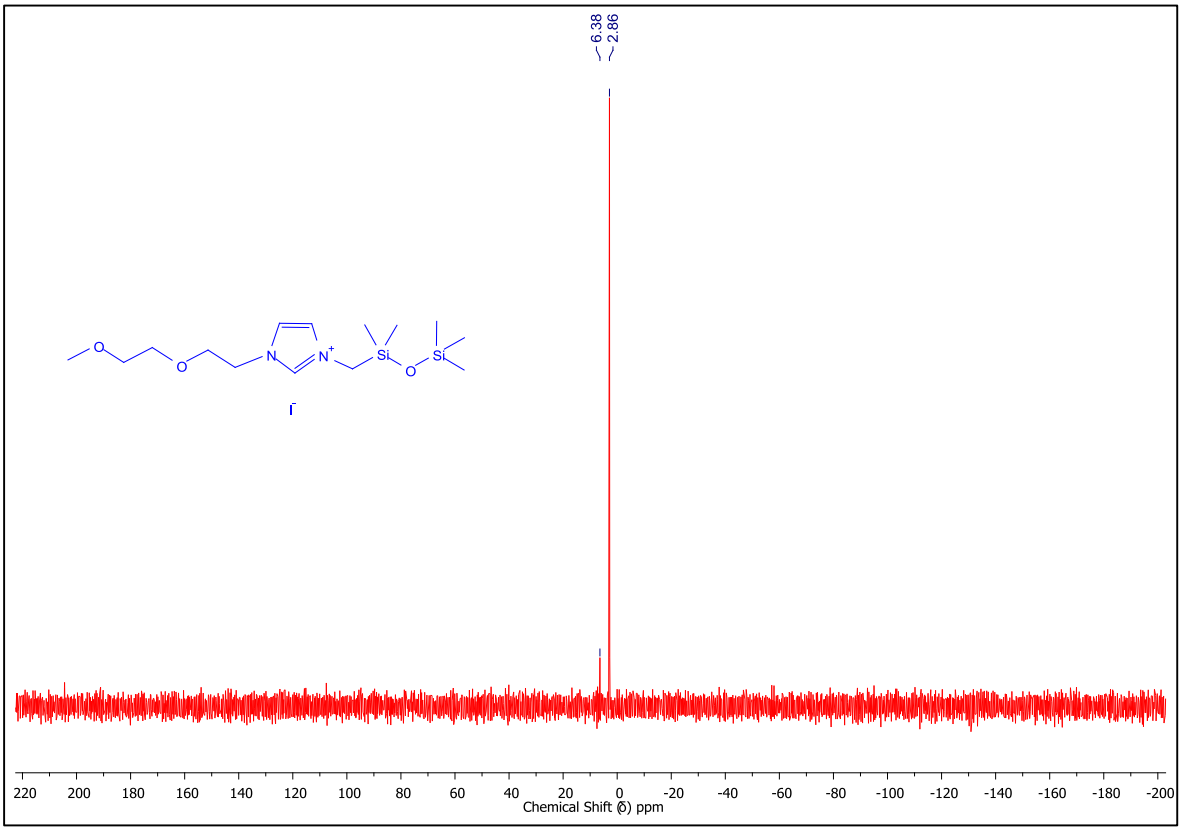

Figure S29: $^{29}Si\{^{1}H\}$ NMR spectrum of compound **2a** in $CDCl_3$

Compound 3a

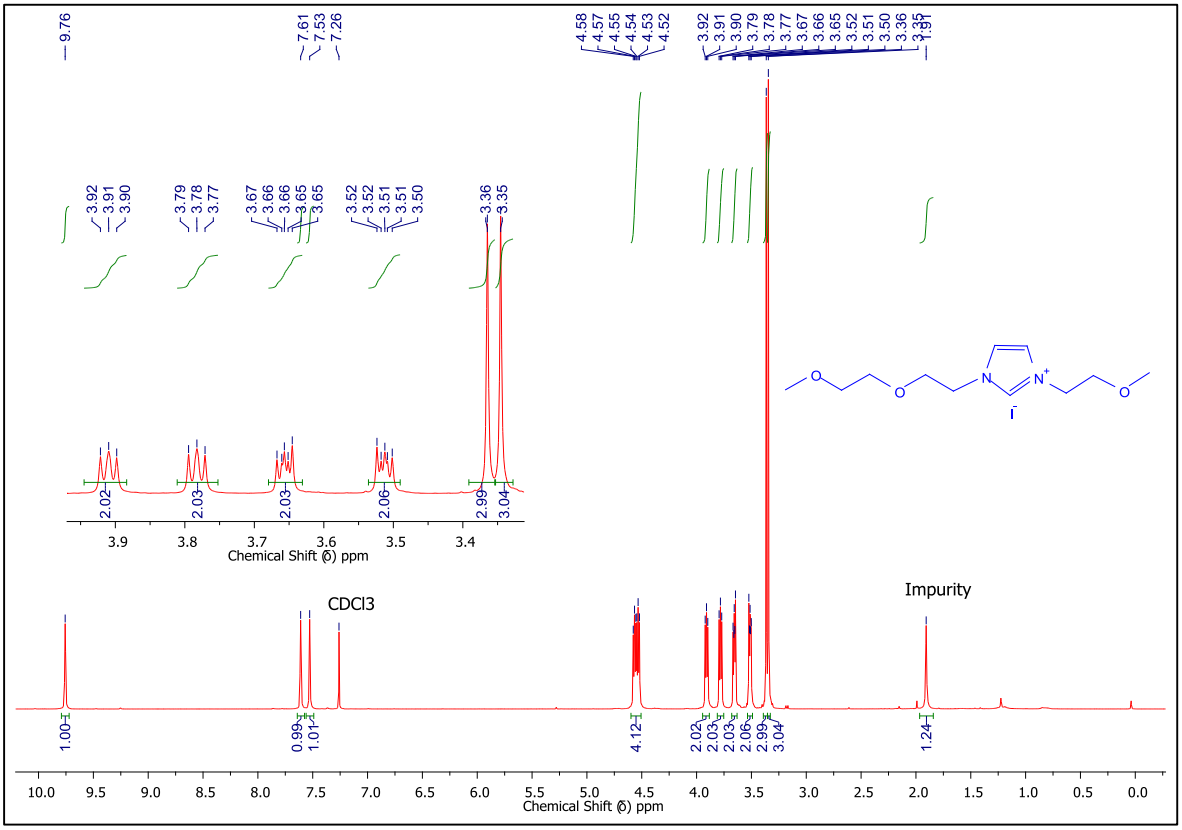

Figure S30: ^{1}H NMR spectrum of compound **3a** in $CDCl_3$

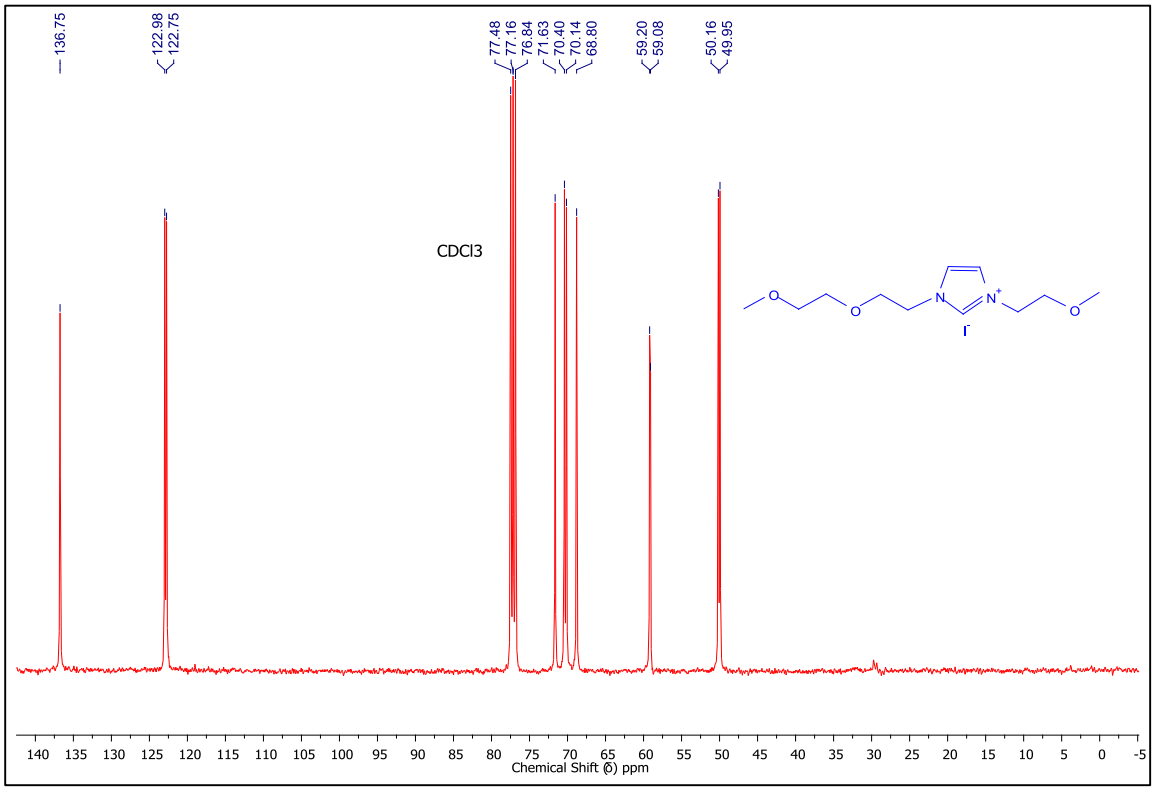

Figure S31: ^{13}C {^{1}H} NMR spectrum of compound **3a** in $CDCl_3$

Compound 4a.

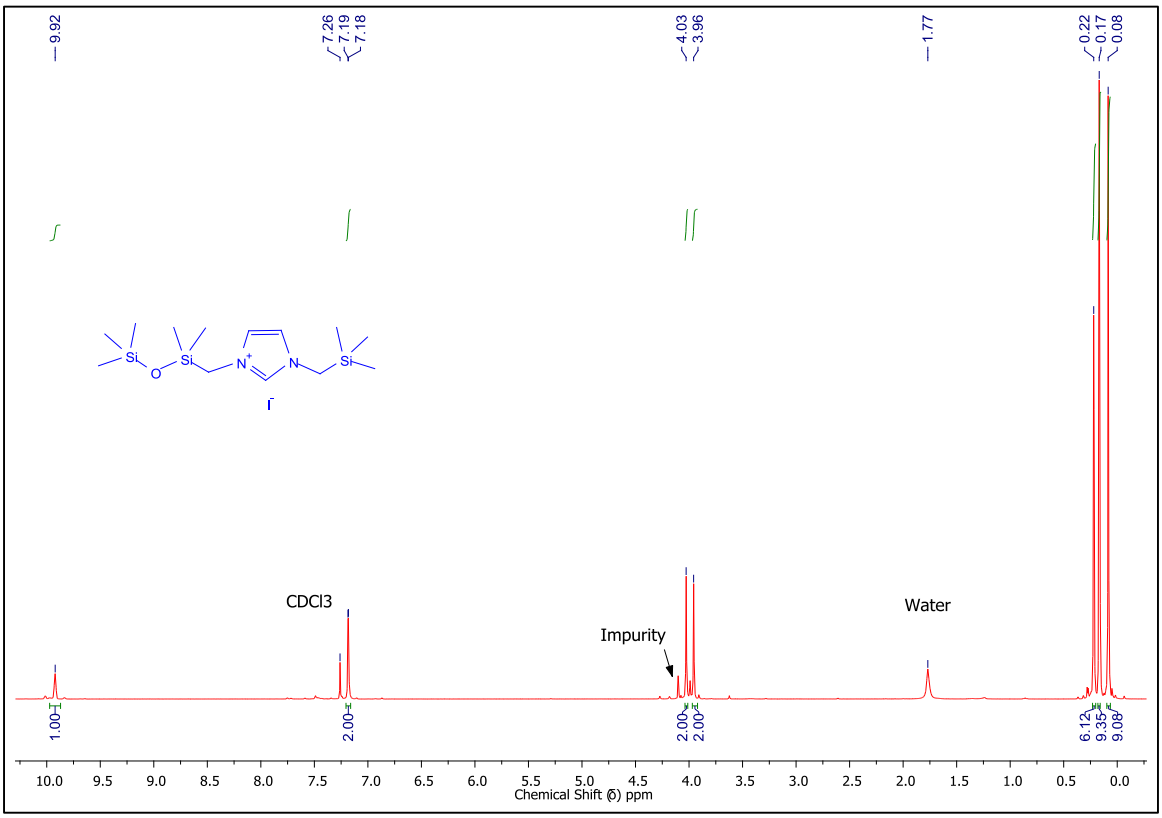

Figure S32: ^{1}H NMR spectrum of compound **4a** in $CDCl_3$

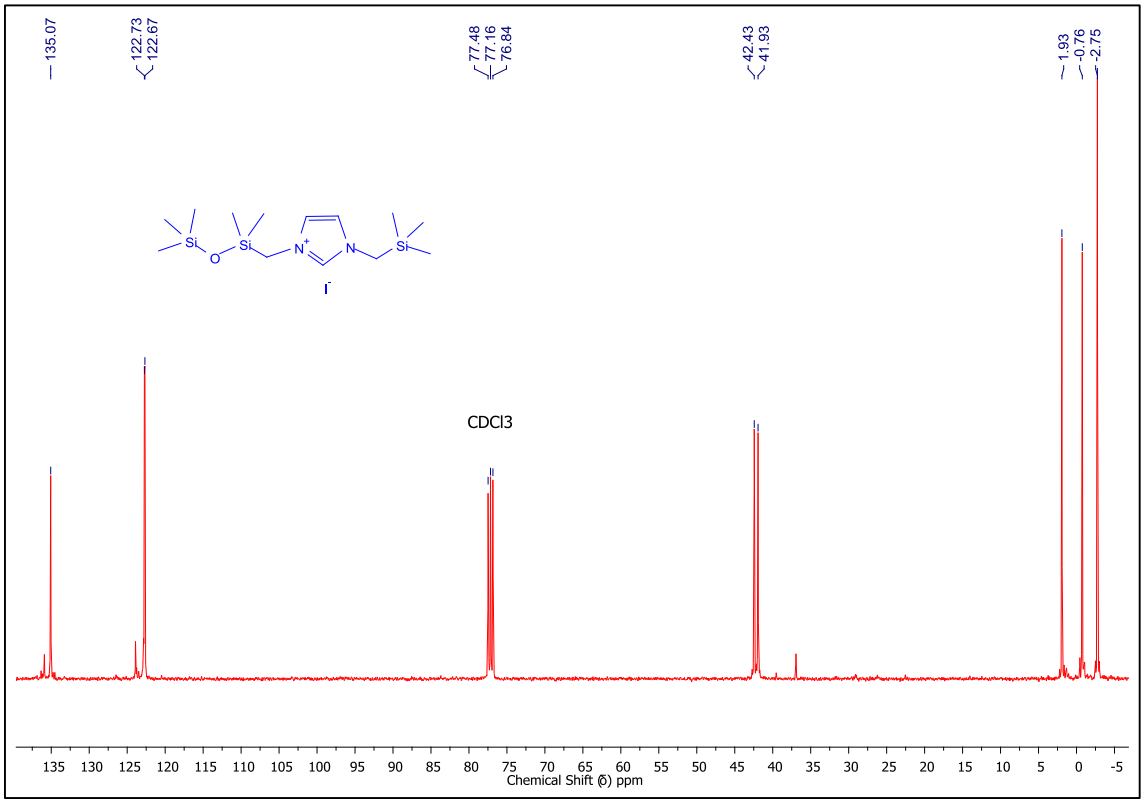

Figure S33: $^{13}C\{^{1}H\}$ NMR spectrum of compound **4a** in $CDCl_3$

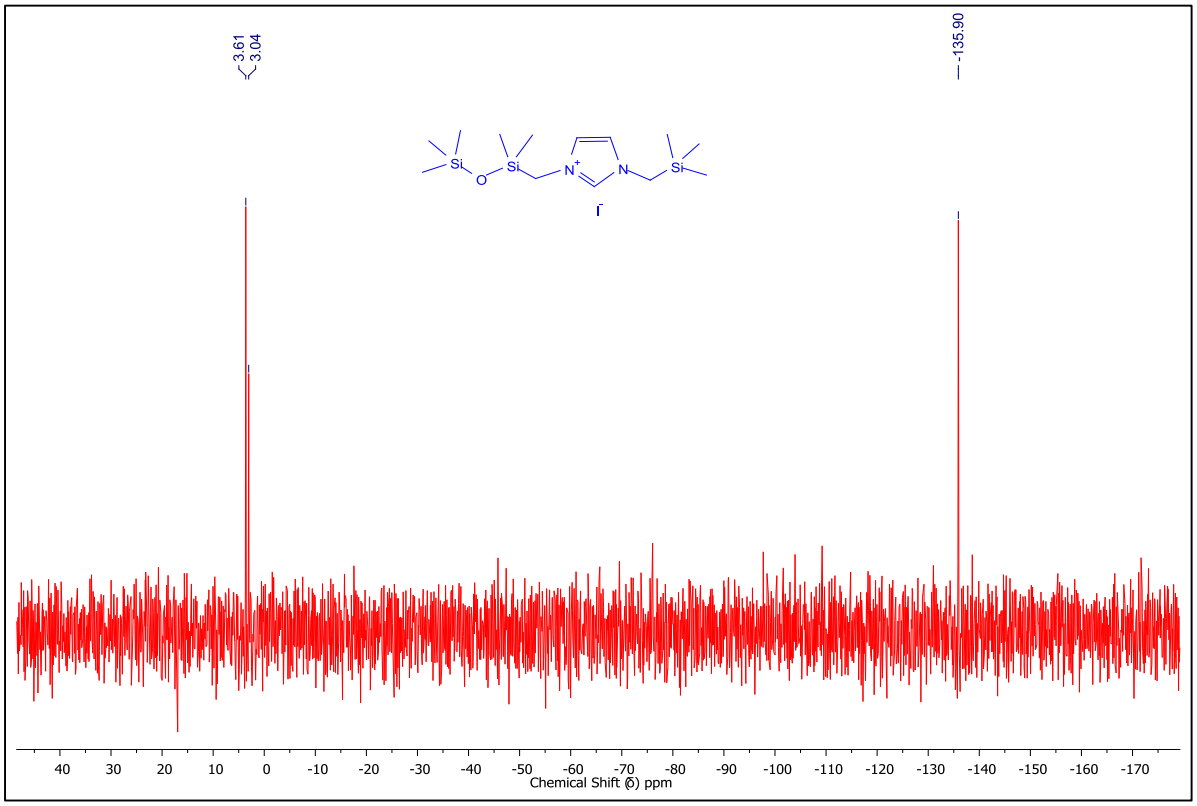

Figure S34: $^{29}Si\{^{1}H\}$ NMR spectrum of compound **4a** in $CDCl_3$

Compound 1b.

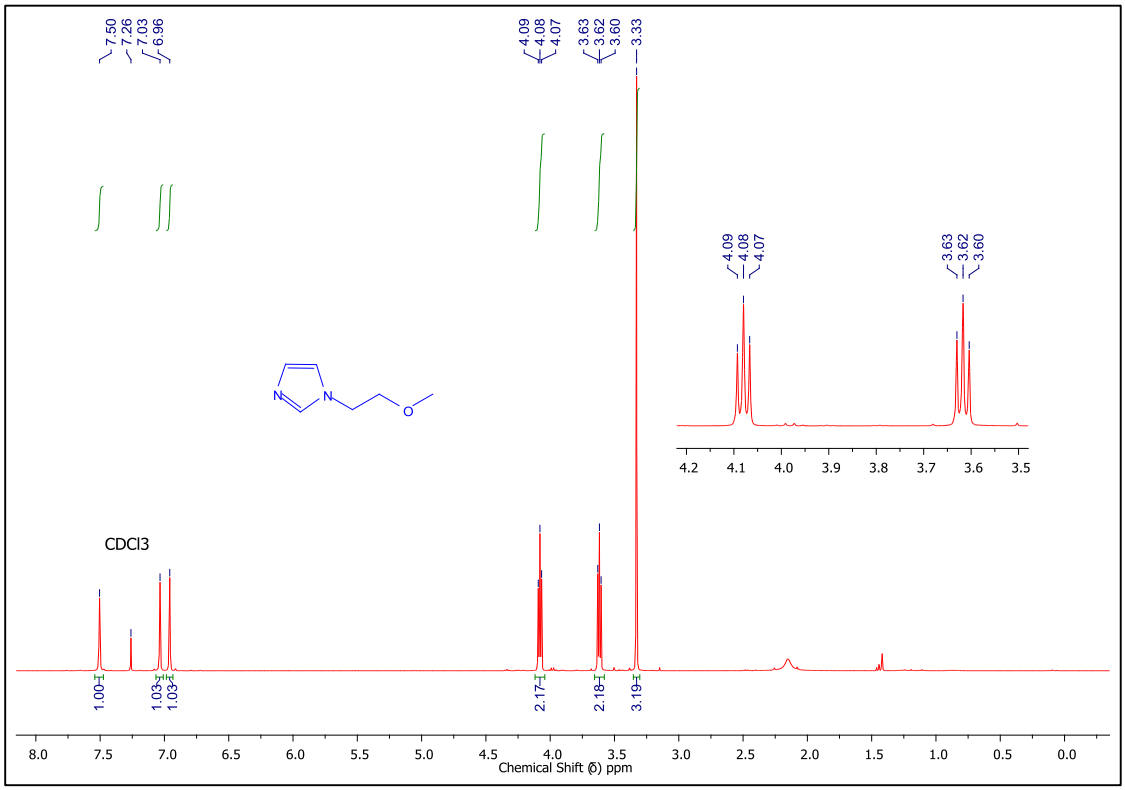

Figure S35: ^{1}H NMR spectrum of compound **1b** in $CDCl_3$

Compound 2b.

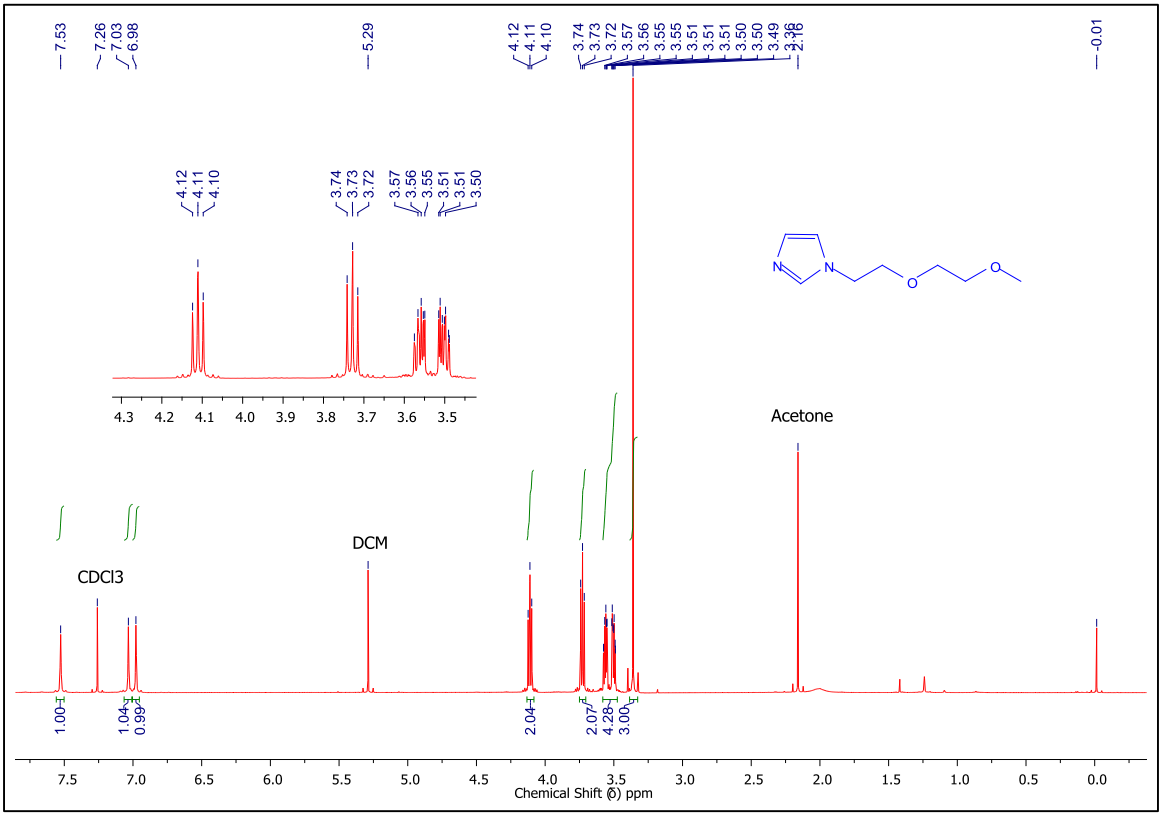

Figure S36: ^{1}H NMR spectrum of compound **2b** in $CDCl_3$

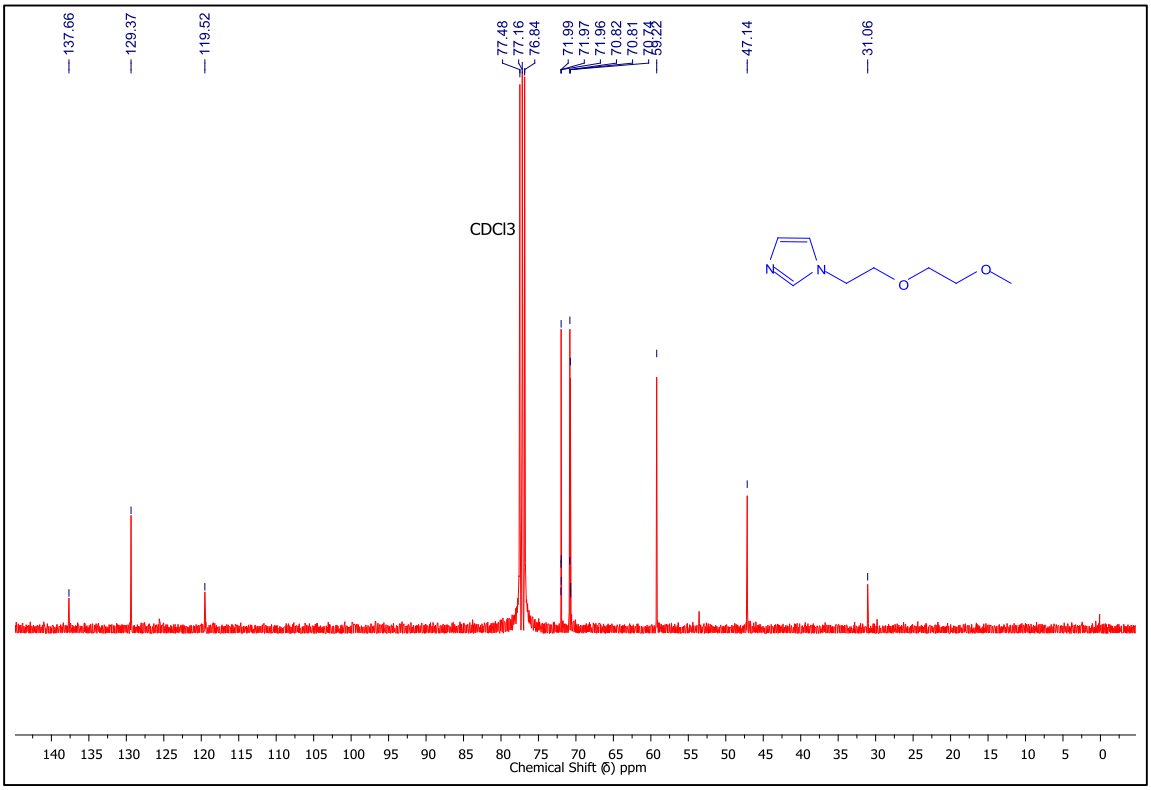

Figure S37: $^{13}C\{^{1}H\}$ NMR spectrum of compound **2b** in $CDCl_3$

Compound 4b.

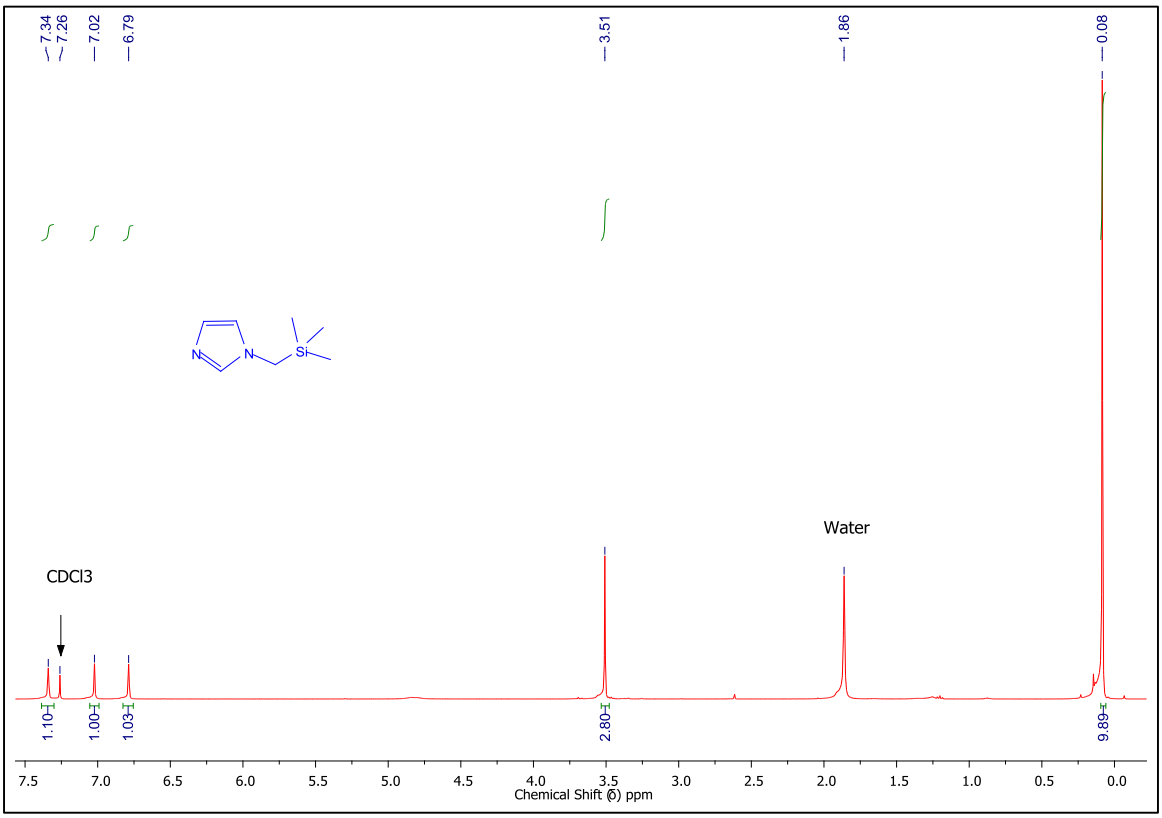

Figure S38: ^{1}H NMR spectrum of compound **4b** in $CDCl_3$

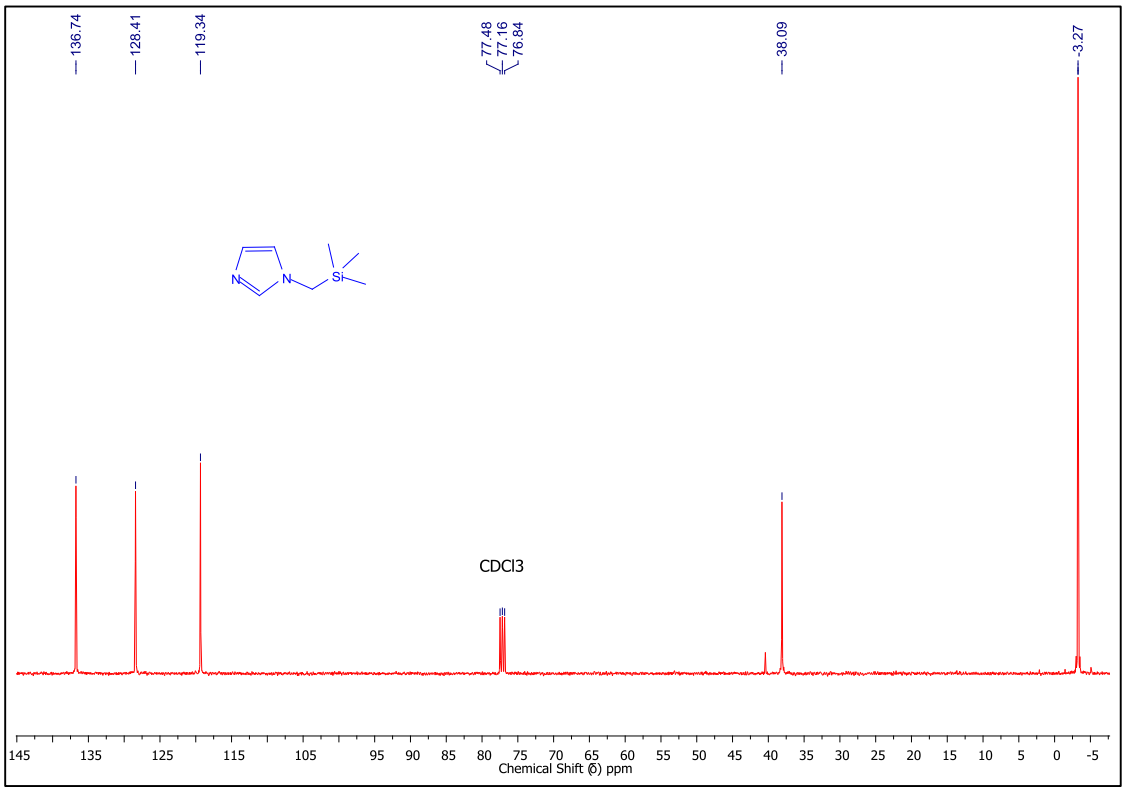

Figure S39: $^{13}C\{^{1}H\}$ NMR spectrum of compound **4b** in $CDCl_3$

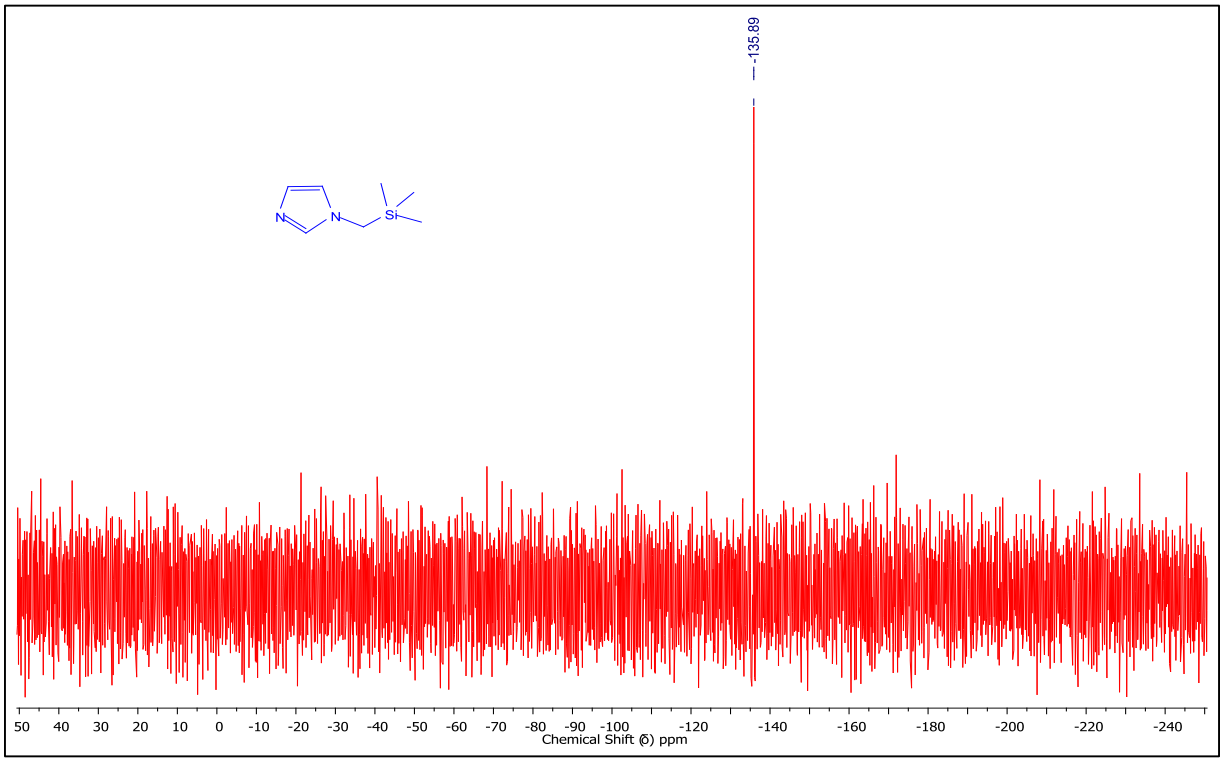

Figure S40: $^{29}Si\{^{1}H\}$ NMR spectrum of **4b** in $CDCl_3$

Compound 6.

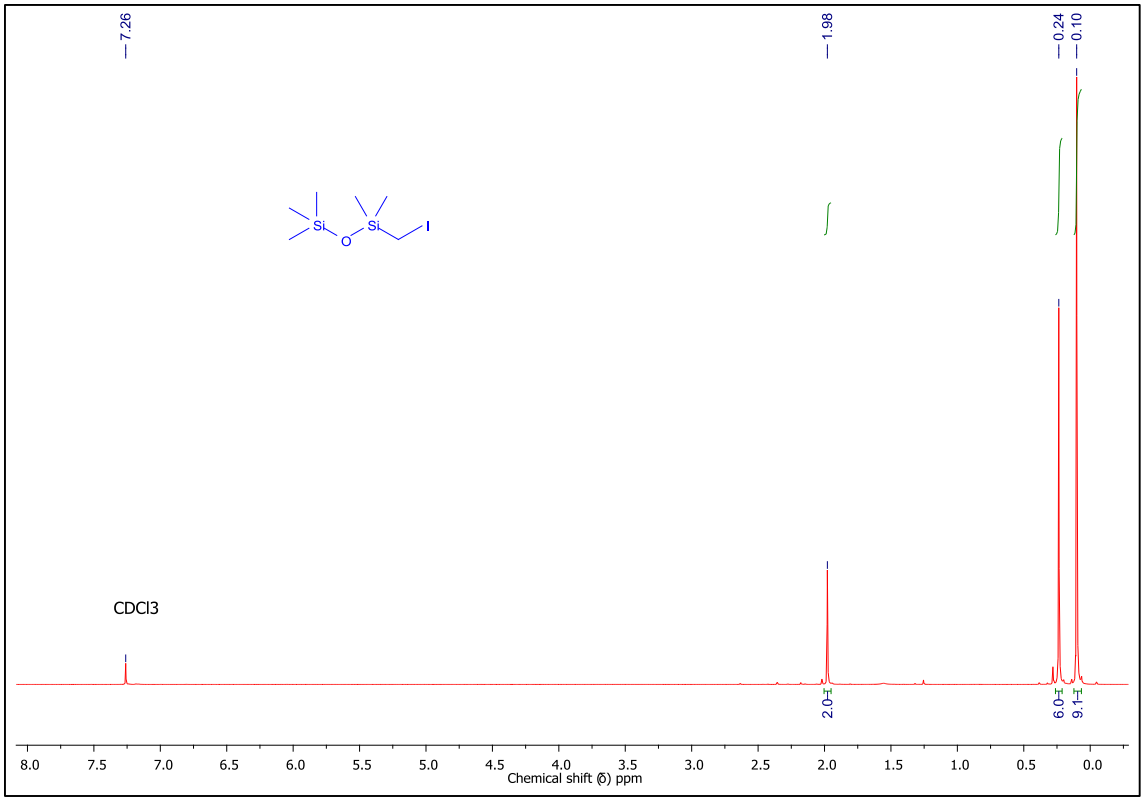

Figure S41: ^{1}H NMR spectrum of compound **6** in $CDCl_3$

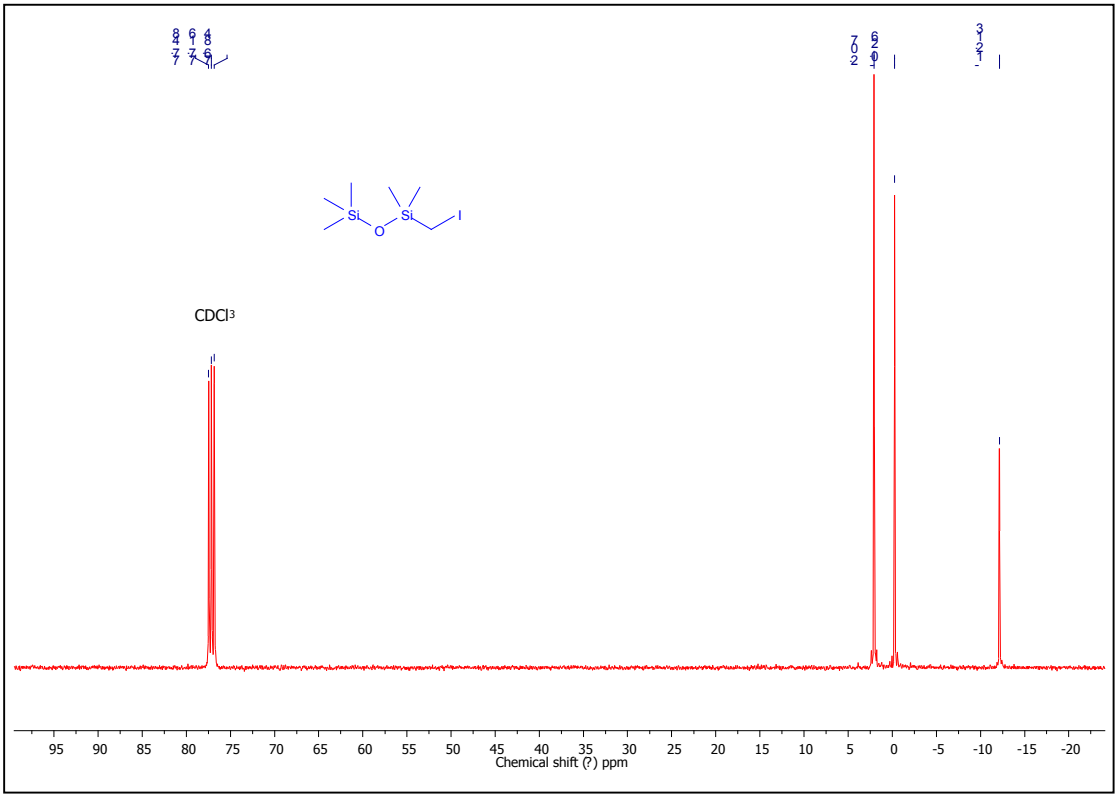

Figure S42: ^{13}C {^{1}H} NMR spectrum of compound **6** in $CDCl_3$

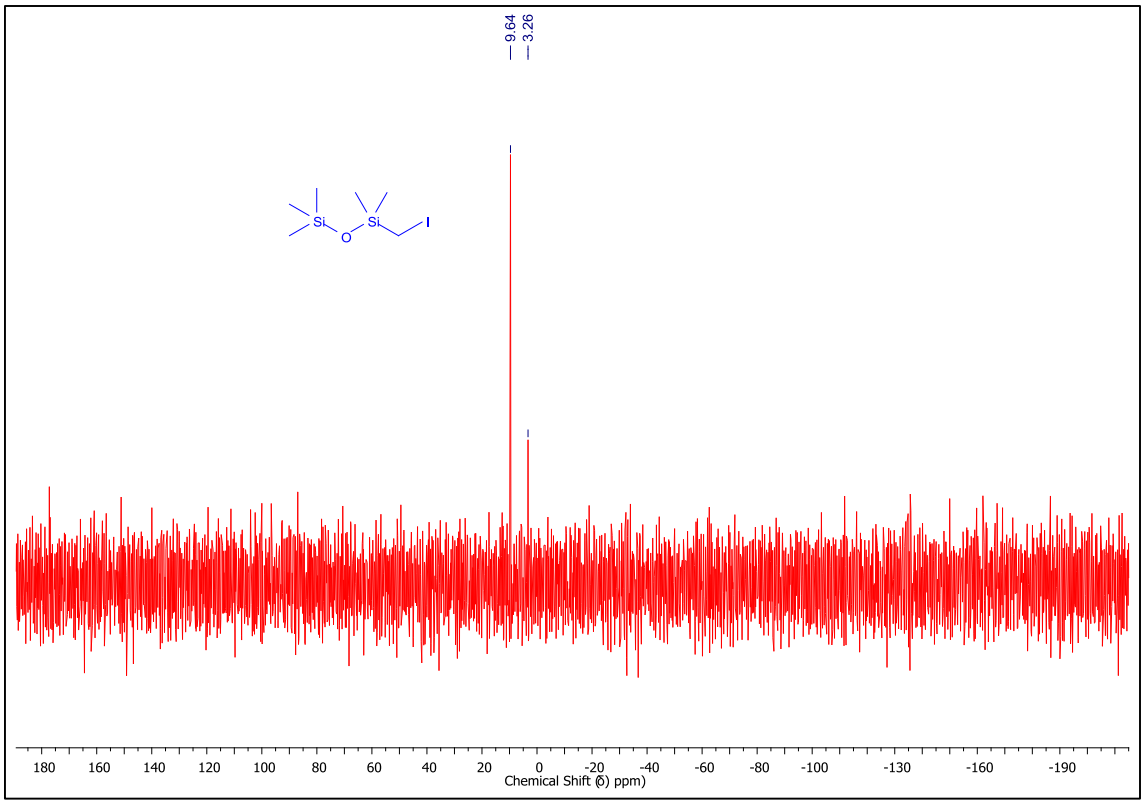

Figure S43: ^{29}Si {^{1}H} NMR spectrum of compound **6** in $CDCl_3$

Compound 8.

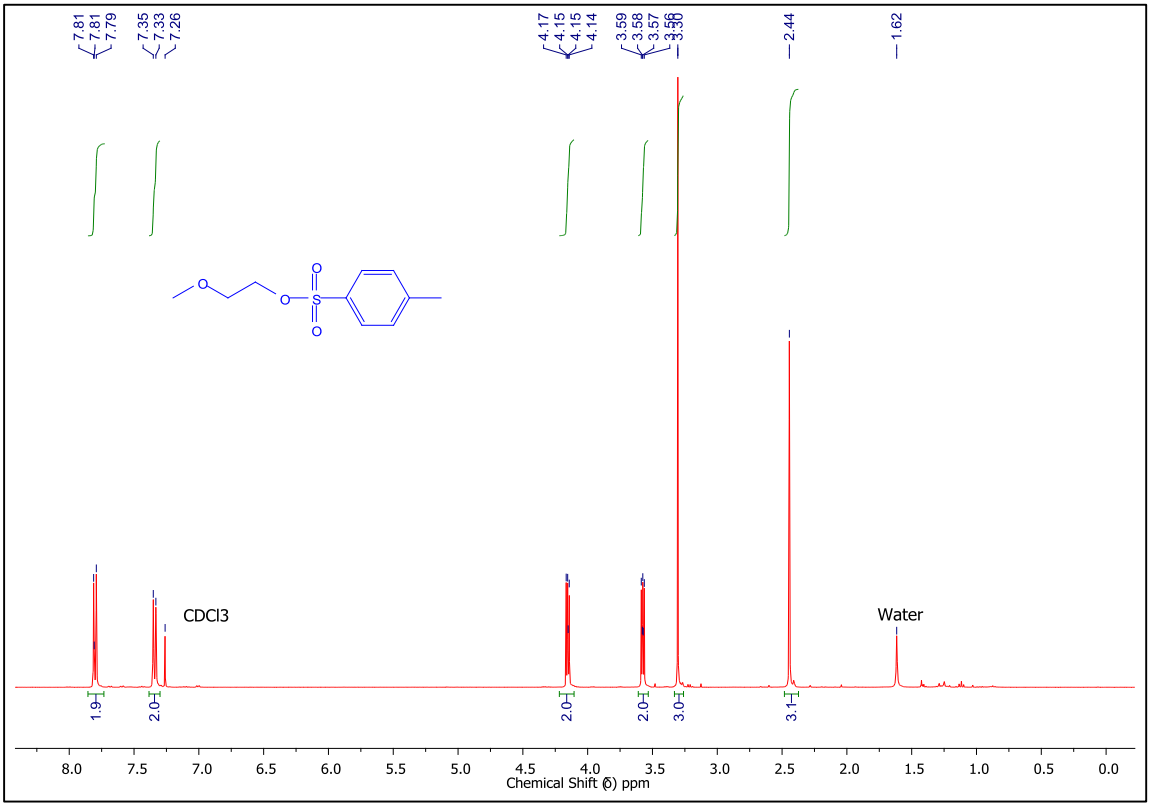

Figure S44: ^{1}H NMR spectrum of compound **8** in $CDCl_3$

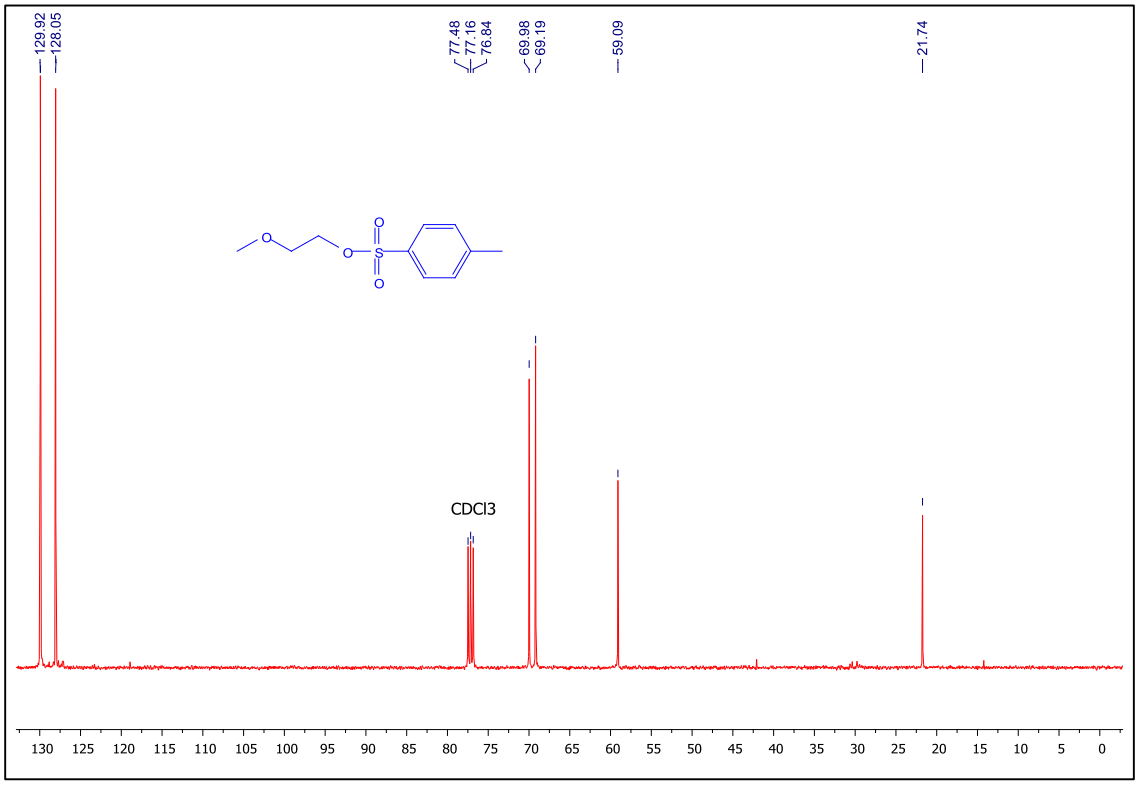

Figure S45: ^{13}C $\{^{1}H\}$ NMR spectrum of compound **8** in $CDCl_3$

Compound 9.

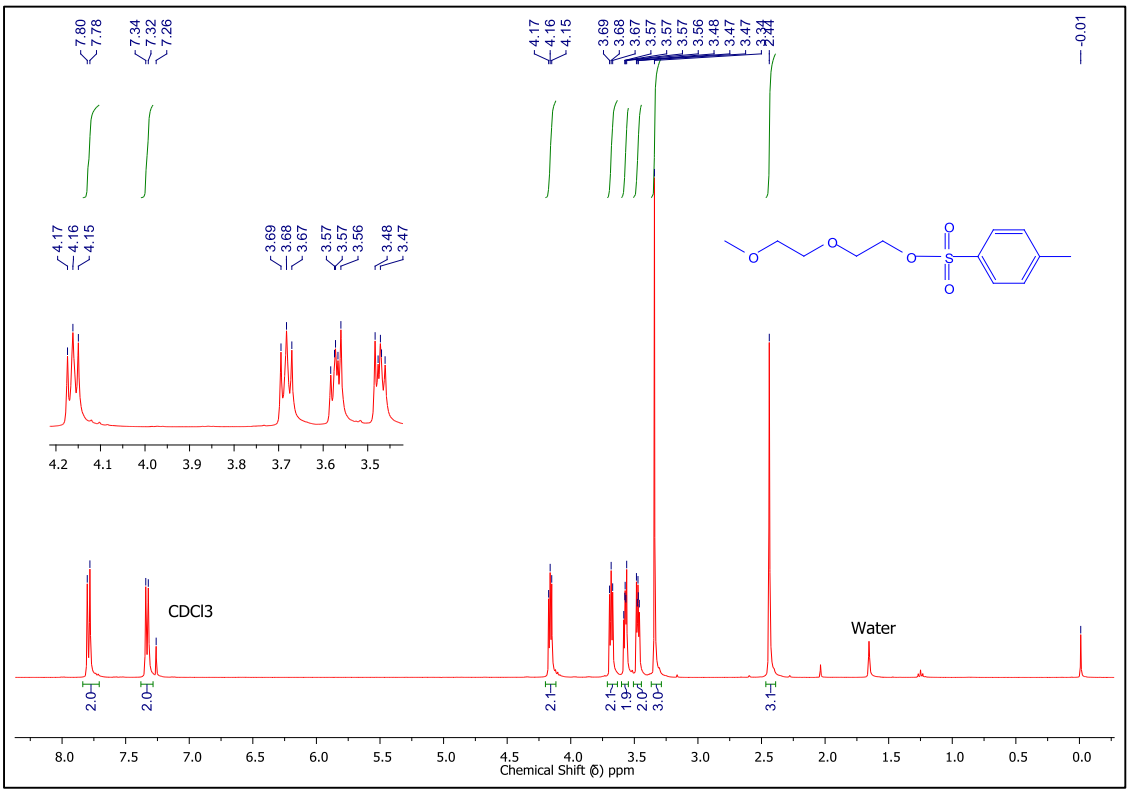

Figure S46: ^{1}H NMR spectrum of compound **9** in $CDCl_3$

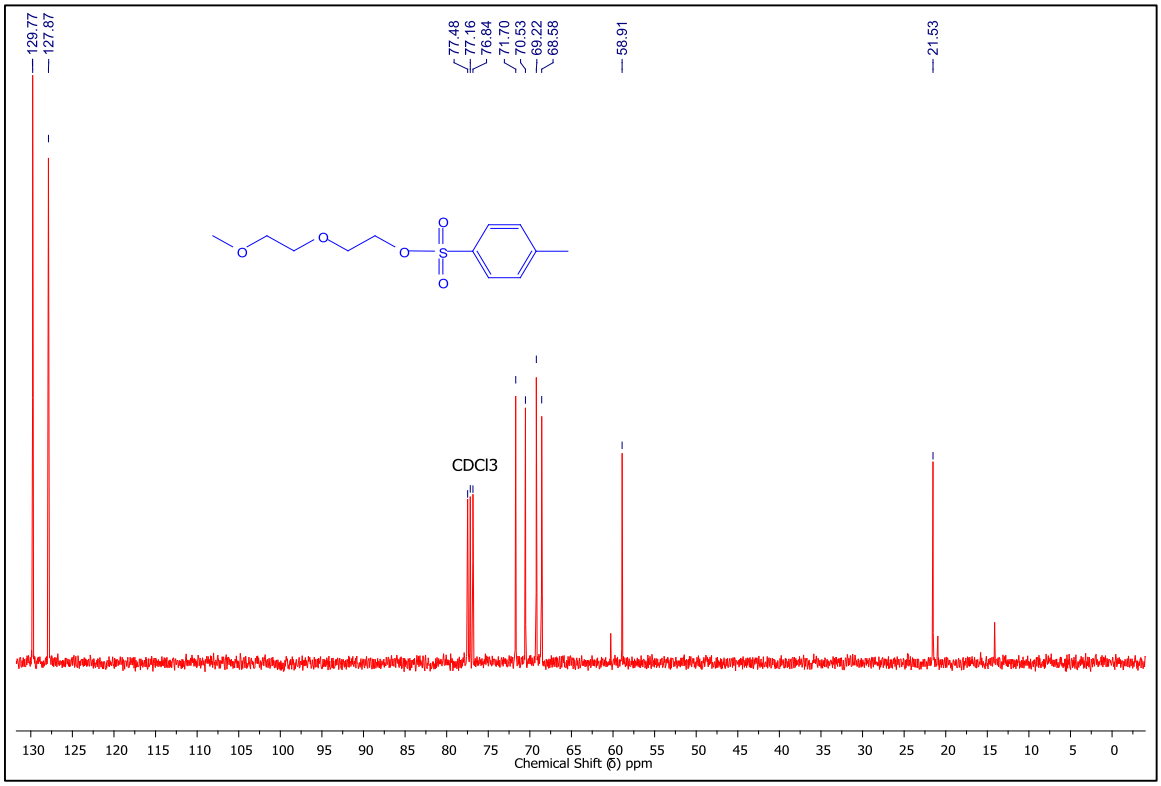

Figure S47: $^{13}C\{^{1}H\}$ NMR spectrum of compound **9** in $CDCl_3$

Compound 10.

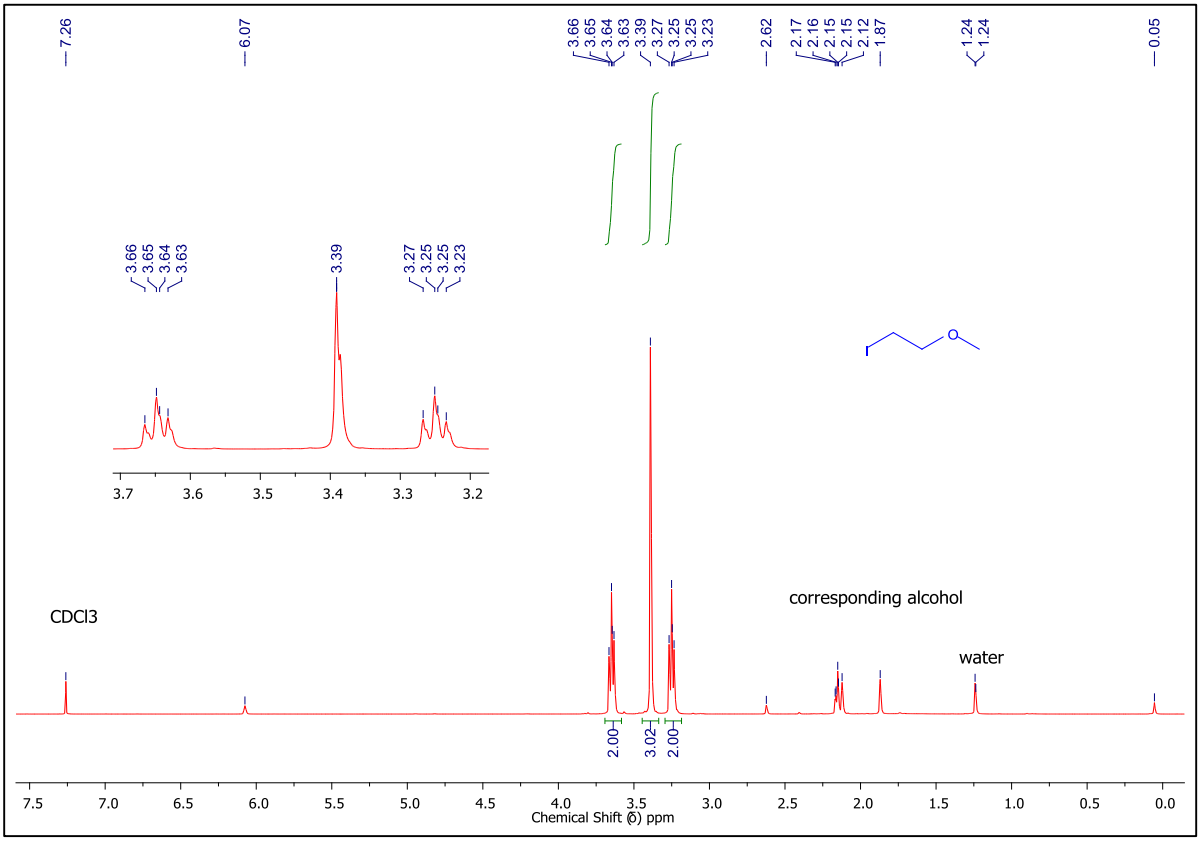

Figure S48: ^{1}H NMR spectrum of compound **10** in $CDCl_3$

References

1. R. H. Krieble and J. R. Elliott, *J. Am. Chem. Soc.* **1945**, *67*, 1810-1812.
2. W. Weng, Z. Zhang, J. Lu and K. Amine, *Chem. Commun.* **2011**, *47*, 11969-11971.
3. M. G. Gichinga and S. Striegler, *Tetrahedron* **2009**, *65*, 4917-4922.
4. M. Döbbelin, I. Azcune, M. Bedu, A. Ruiz de Luzuriaga, A. Genua, V. Jovanovski, G. Cabañero and I. Odriozola, *Chem. Mater.* **2012**, *24*, 1583-1590.
5. J. E. Bara, C. J. Gabriel, S. Lessmann, T. K. Carlisle, A. Finotello, D. L. Gin and R. D. Noble, *Ind. Eng. Chem. Res.* **2007**, *46*, 5380-5386.
6. J. Yuan and M. Antonietti, *Polymer* **2011**, *52*, 1469-1482.
7. H. Shirota, J. F. Wishart and E. W. Castner, *J. Phys. Chem. B* **2007**, *111*, 4819-4829.